Journal of Autoimmunity 102 (2019) 50–64

Contents lists available at ScienceDirect

Journal of Autoimmunity

journal homepage: www.elsevier.com/locate/jautimm

Interleukin-1β-induced IRAK1 ubiquitination is required for T_H-GM-CSF cell differentiation in T cell-mediated inflammation

Yuan Hu[a,b,1], Feihong Xu[a,1], Ruihua Zhang[a], Diana Legarda[a], Jun Dai[a,b], Di Wang[a], Heyu Li[a], Yao Zhang[c], Qingjie Xue[a,b], Guanjun Dong[b], Hui Zhang[a,b], Chang Lu[d], Arthur Mortha[a], Jianguo Liu[e], Paolo Cravedi[f], Adrian Ting[a], Liwu Li[c], Chen-feng Qi[g], Susan Pierce[g], Miriam Merad[a], Peter Heeger[f,**], Huabao Xiong[a,b,*]

[a] Department of Medicine, Precision Immunology Institute, Icahn School of Medicine at Mount Sinai, New York, NY, 10029, USA
[b] Institute of Immunology and Molecular Medicine, Jining Medical University, Shandong, 272067, China
[c] Department of Biological Sciences, Virginia Tech, Blacksburg, VA, 24061, USA
[d] Department of Biomedical Engineering, Virginia Tech, Blacksburg, VA, 24061, USA
[e] Departments of Internal Medicine & Molecular Microbiology and Immunology, Saint Louis University School of Medicine, St. Louis, MO, 63104, USA
[f] Department of Medicine, Translational Transplant Research Center, Icahn School of Medicine at Mount Sinai, New York, NY, 10029, USA
[g] Laboratory of Immunogenetics, National Institute of Allergy and Infectious Diseases, National Institutes of Health, Bethesda, MD, 20892, USA

A B S T R A C T

Accumulating evidence suggests granulocyte macrophage-colony stimulating factor (GM-CSF) can function as an inflammatory mediator, but whether GM-CSF-producing $CD4^+$ T cells (T_H-GM-CSF) are a distinct T helper cell subset is lacking. Herein we demonstrate that interleukin (IL)-1β exclusively drives differentiation of naïve $CD4^+$ T cells into T_H-GM-CSF cells via inducing ubiquitination of IL-1 receptor-associated kinase 1 (IRAK1) and subsequent activation of the transcription factor NF-kappaB (NF-κB), independent of RAR-related orphan receptor gamma (RORγt) required for T_H17 differentiation. *In vivo,* T_H-GM-CSF cells are present in murine *Citrobacter Rodentium* infections and mediate colitis following adoptive transfer of $CD4^+$ T cells into *Rag1*$^{-/-}$ mice via GM-CSF-induced macrophage activation. The T_H-GM-CSF cell phenotype is stable and distinct from the T_H17 genetic program, but IL-1β can convert pre-formed T_H17 cells into T_H-GM-CSF cells, thereby accounting for previously reported associations between IL-17 and GM-CSF. Together, our results newly identify IL-1β/NF-κB-dependent T_H-GM-CSF cells as a unique T helper cell subset and highlight the importance of $CD4^+$ T cell-derived GM-CSF induced macrophage activation as a previously undescribed T cell effector mechanism.

1. Introduction

Granulocyte macrophage-colony stimulating factor (GM-CSF) was initially identified as a hematopoietic growth factor [1] but emerging evidence indicates that beyond myelopoiesis, GM-CSF can exert pro-inflammatory effects [2–4]. GM-CSF is produced by a number of cell types including T cells, B cells, monocytes/macrophages among other sources [3,5–8], but whether and how GM-CSF produced by each of these cell types impacts immune responses to pathogens and/or auto-antigens remains to be elucidated.

T helper cell production of GM-CSF has been shown to participate in the pathogenesis of various autoimmune diseases and animal models. For example, in experimental autoimmune encephalomyelitis (EAE), the ability of activated T helper cells to produce GM-CSF renders them functionally mature and pathogenic, leading to the activation of downstream effector cells and as a consequence, the propagation of inflammation [9–12]. $GM\text{-}CSF^+CD4^+$ T cells that do not express IL-17 or IFN-γ are present in the inflammatory sites of EAE [9,14,15] and $CD4^+$ T cells deficient in GM-CSF, but not in interferon (IFN)-γ and/or interleukin (IL)-17 failed to induce EAE [9,10]. Together with the observation that GM-CSF producing T cells are detectable in multiple sclerosis (MS) patients [16,17] these published findings suggest a non-redundant role for GM-CSF-producing $CD4^+$ T cells in these CNS autoimmune disease processes.

Although many factors have been shown to induce GM-CSF production in T cells, no definite conclusion has yet been reached

* Corresponding author. Precision Immunology Institute, Box 1630, Icahn School of Medicine at Mount Sinai, 1 Gustave L. Levy Place, New York, NY, 10029-6574, USA.
** Corresponding author. Department of Medicine, Translational Transplant Research Center, Icahn School of Medicine at Mount Sinai, 1 Gustave L. Levy Place, New York, NY, 10029-6574, USA.
E-mail addresses: peter.heeger@mssm.edu (P. Heeger), Huabao.Xiong@mssm.edu (H. Xiong).
[1] Equally contributed to the research.

https://doi.org/10.1016/j.jaut.2019.04.010
Received 18 January 2019; Received in revised form 12 April 2019; Accepted 12 April 2019
Available online 10 May 2019
0896-8411/

regarding which T helper subset is the predominant producer of GM-CSF. Published studies have proposed that both IL-17-producing T helper cells (T_H17) and type 1 T helper cells (T_H1) can express GM-CSF in response to certain stimuli, including IL-23 or IL-1β [10,13]. *In vitro* stimulation of preformed IL-17$^+$GM-CSF$^-$ T_H17 cells with IL-23 and IL-1β converted of a subset of these IL-17-producers into a population of GM-CSF$^+$IL-17$^-$IFN-γ$^-$CD4$^+$ T cells, which by definition are not either T_H17 or T_H1[10]. These observations highlight the complexity of T helper cell lineage differentiation and raise a question of whether GM-CSF-producing CD4$^+$ T cells represent a stable lineage separate from previously identified T helper subsets. To date, only one study has partially addressed this issue, by demonstrating signal transducer and activator of transcription 5 (STAT5) signaling is uniquely required for CD4$^+$ T cell differentiation into GM-CSF producers [11]. The characterized phenotype, regulatory circuits of GM-CSF-producing CD4$^+$ T cells and their cellular targets, and potential effects these cells may have with regard to immune responses have yet to be delineated.

Herein, we provide unequivocal evidence that GM-CSF-producing CD4$^+$ T cells (T_H-GM-CSF) are a unique T helper cell subset is distinct from T_H17 cells. We show that IL-1β directly programs GM-CSF production in naïve CD4$^+$ T cells via interleukin-1 receptor-associated kinases 1 (IRAK1)-initiated activation of the transcription factor NF-kappaB (NF-κB) and that IL-1β induces conversion of IL-17 producers into T_H-GM-CSF cells. We also show that T_H-GM-CSF cells and the T_H17 to T_H-GM-CSF trans-differentiation crucially mediates colitis induced by adoptive transfer of naïve CD4$^+$ T cells into *Rag1*$^{-/-}$ mice. Together with experiments demonstrating GM-CSF-induced macrophage activation as contributing to the development of colitis our findings shed new light on the differentiation program of T helper cells and uncover the mechanisms that govern their lineage commitment and function.

2. Results

2.1. IL-1β-elicited GM-CSF-producing CD4$^+$ T cells are unique T helper cells

Building upon published observations that IL-1β and IL-23 upregulate GM-CSF expression under T_H17 polarization conditions [9,18] we investigated whether IL-1β and/or IL-23 directly program GM-CSF production in naïve precursors to produce GM-CSF, independent of IL-17-inducing TGF-β and IL-6. We purified naïve CD4$^+$ T cells from the spleen and lymph nodes of B6 (WT) mice and stimulated them *in vitro* for three days in the presence of various cytokines (Fig. 1a). We observed that whereas cells treated with IL-1β alone produced significant quantities of GM-CSF without IL-17A in a dose dependent manner, cells treated with IL-23 alone (regardless of concentration added) and cells cultured under T_H0 conditions generated only small amounts of GM-CSF (Fig. 1a and Supplementary Fig. 1a). The combination of IL-1β and IL-23 did not increase T cell GM-CSF production above that induced by IL-1β alone (Fig. 1a). In control experiments, classical T_H17 polarizing conditions (TGF-β and IL-6) yielded essentially no GM-CSF (Fig. 1a). ELISAs performed on culture supernatants confirmed a substantial augmentation of GM-CSF secretion with minimal IL-17A production in cells differentiated in the presence of IL-1β while supernatants of cells cultured with TGF-β/IL-6 produced IL-17A without GM-CSF (Fig. 1b and Supplementary Figs. 1b and c).

To verify that IL-1β/IL-1 receptor ligations on the responding T cells are essential for GM-CSF production by T helper cells, we purified naïve CD4$^+$ T cells from WT and IL-1 receptor knockout (*IL1R1*$^{-/-}$) mice and primed them *in vitro* for three days under T_H0 conditions or in the presence of IL-1β. These assays showed lack of CD4$^+$ T cell-expressed IL-1 receptor prevented the induction of GM-CSF-producing CD4$^+$ T cells, resulting in low level GM-CSF production similar to that observed in under control T_H0 conditions (Fig. 1c and d). To test the lineage stability of T_H-GM-CSF, we differentiated naïve CD4$^+$ T cells with IL-1β for 12 days and observed continued stable GM-CSF production with a peak GM-CSF expression at day 6 (Supplementary Fig. 1d), arguing against previous suggestions that transient GM-CSF production is a component of the T_H17 program [19,20]. In specificity control experiments we observed that naïve CD4$^+$ T cells cultured under conditions that guide differentiation toward T_H1, T_H2, T_{FH} or Treg produced minimal amount of GM-CSF (intracellular and by ELISA, Fig. 1e and f).

Together these results support the conclusion that IL-1β elicits T_H-GM-CSF cells that are distinct from classical T_H17 cells and other T helper cell subsets described previously, and thus represent a unique T helper cell subset.

To begin to explore the *in vivo* function of T_H-GM-CSF, we challenged WT mice by oral inoculation with *Citrobacter Rodentium* to induce colitis and performed kinetic immune-phenotyping of the infected mice. One week after infection we observed clear proportions of IL-17A- and IFN-γ-producing cells in the spleens and mesenteric lymph nodes (MLNs) (Fig. 1g and h), which is consistent with previous findings showing that T_H1 and T_H17 cytokines are critical for host defense against *Citrobacter Rodentium*. We also observed a distinct population of GM-CSF single positive CD4$^+$ T cells, with no GM-CSF$^+$IL-17A$^+$ or GM-CSF$^+$IFN-γ$^+$ cells (Fig. 1g and h). In addition, at two weeks post-infection we observed sharp decreases in the proportions of IL-17A- and IFN-γ-producing cells. Meanwhile, the percentage of GM-CSF single positive cells increased significantly in the spleens and MLNs without detectable GM-CSF$^+$IL-17A$^+$ or GM-CSF$^+$IFN-γ$^+$ cells existing (Fig. 1g and h). Together the data support the conclusion that T_H-GM-CSF cells can develop *in vivo* and mediate mucosal inflammation independent of other T helper subsets.

2.2. T_H17 cells possess plasticity to convert into T_H-GM-CSF cells

As T_H17 cells can differentiate into other T helper cell types upon the appropriate stimuli [21–24] and previous work by others indicated that T cell production of GM-CSF is IL-23 and RAR-related orphan receptor gamma (RORγt)-dependent, we next tested the hypothesis that IL-1β and/or IL-23 induces T_H17 cells to produce GM-CSF [10]. We cultured naïve CD4$^+$ T cells with TGF-β plus IL-6, and then restimulated them either without cytokines or with IL-1β/IL-23, among other combinations of cytokines (Fig. 2a). These assays revealed a) the percentage of IL-17A single producing cells decreased in all conditions tested (Fig. 2a) and b) IL-1β + IL-23 induced a small fraction of IL-17A$^+$GM-CSF$^+$CD4$^+$ T cells (Fig. 2a). Notably, in these re-stimulations, IL-1β alone or together with IL-23 resulted in a considerable increase in the proportion of GM-CSF single producing cells, and enhanced clonal expansion, whereas either TGF-β plus IL-6 or IL-23 alone had negligible effects (Fig. 2a and Supplementary Fig. 2a). We additionally observed more GM-CSF production in the IL-1β or IL-1β/IL-23 restimulated T_H17 cells than in T_H-GM-CSF differentiated directly from naïve CD4$^+$ T cells (Fig. 2b). These data support IL-1β as a crucial transdifferentiation signal that switches the T_H17 phenotype to a T_H-GM-CSF phenotype. These *in vitro* results further indicate that T_H-GM-CSF cells can derive directly from naïve CD4$^+$ cells or can transdifferentiate from T_H17 cells, the latter providing an explanation for previously reported associations between the T_H17 lineage and GM-CSF production.

In control experiments, we tested whether IL-1β induces the conversion toward T_H-GM-CSF phenotype from committed T_H1 and Treg cells and found that re-stimulations in both cell types produced undetectable amounts of GM-CSF (Fig. 2c and Supplementary Fig. 2b), indicating the switch is specific to T_H17-inducing conditions rather than to global activation of T cells.

To further investigate the T_H17-to-T_H-GM-CSF transdifferentiation *in vivo*, we flow-sorted *in vitro* differentiated CD4$^+$IL-17$^+$-GFP$^+$ T cells from reporter mice and adoptively transferred them into *Rag1*$^{-/-}$ recipients. Two weeks later analyses of splenic T cells showed a distinct population of single, GM-CSF-producing CD4$^+$ T cells in addition to IFN-γ$^+$CD4$^+$ T cells (Fig. 2d), indicating that T_H17 cells possess the

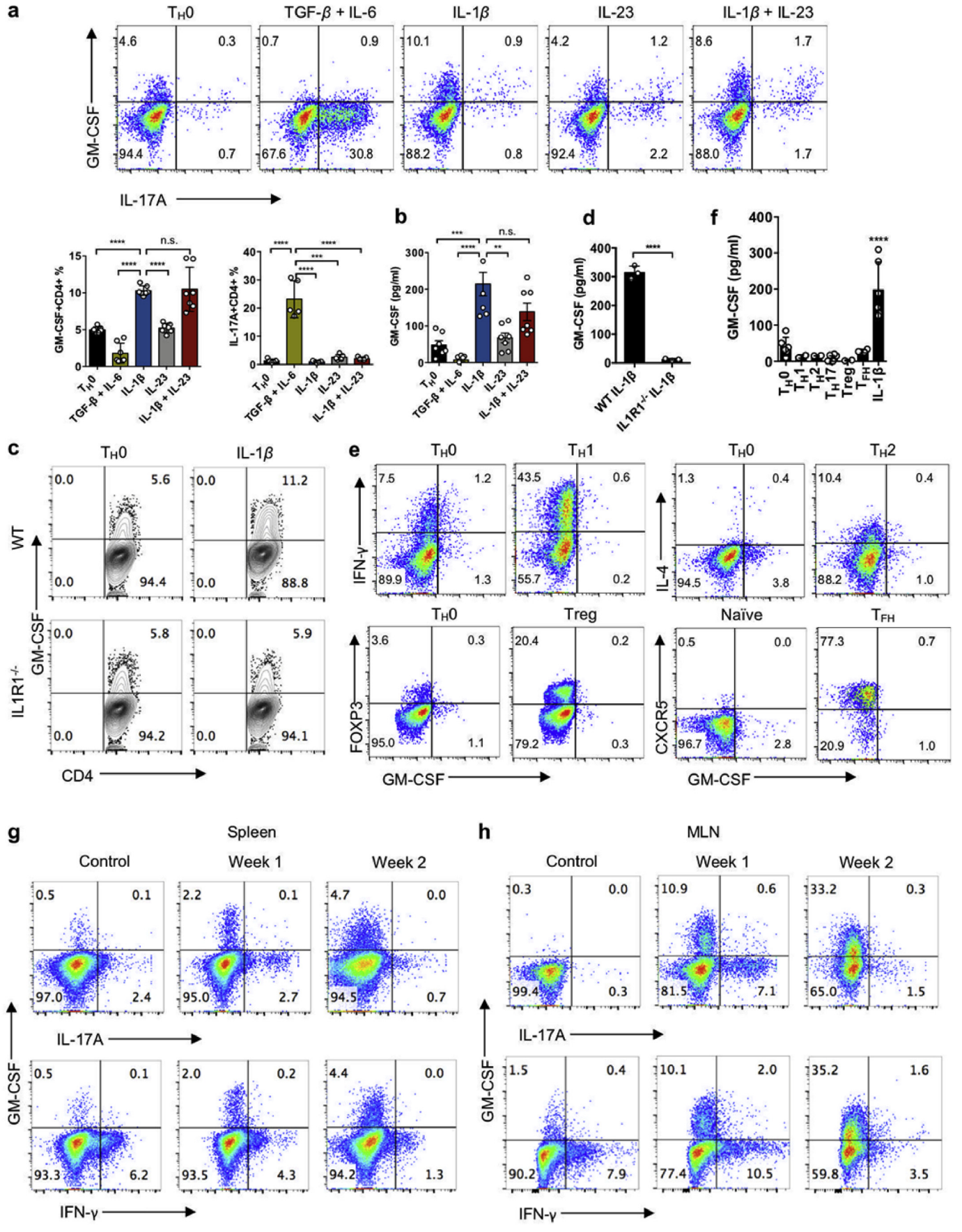

(caption on next page)

Fig. 1. IL-1β-elicited GM-CSF-producing CD4$^+$ T cells are unique T helper cells. (a) Naïve CD4$^+$ T cells from the spleen and lymph nodes of C57BL/6 mice were differentiated *in vitro* for 3 days under T_H0 polarizing condition or in the presence of TGF-β plus IL-6, or IL-1β, or IL-23, or IL-1β plus IL-23. Cells were then restimulated with PMA/ionomycin/monensin for 5 h, stained for intracellular GM-CSF and IL-17A and analyzed by flow cytometry (top: representative dot plot, bottom: means of 7 or 5 independent experiments). (b) Supernatants of cells prepared in (a) were analyzed for GM-CSF by ELISA. (c) Naïve CD4$^+$ T cells from the spleen and lymph nodes of WT and *IL1R1*$^{-/-}$ mice were differentiated *in vitro* for 3 days under T_H0 or in the presence of IL-1β. Cells were then restimulated with PMA/ionomycin/monensin for 5 h, stained for intracellular GM-CSF and analyzed by flow cytometry. (d) Supernatants of cells prepared in (c) were analyzed for GM-CSF by ELISA. (e) Naïve CD4$^+$ T cells from the spleen and lymph nodes of C57BL/6 mice were differentiated *in vitro* for 3 days under T_H0, T_H1, T_H2, Treg and T_{FH} polarizing conditions and were analyzed for GM-CSF expression by flow cytometry. (f) Supernatants of cells prepared in (e), and T_H17 cells and cells cultured with IL-1β were analyzed for GM-CSF secretion by ELISA. (g) and (h) WT mice were challenged by oral inoculation with *Citrobacter Rodentium* for 1 or 2 weeks. At sacrifice, cells from spleens (g) and mesenteric lymph nodes (MLNs) (h) were isolated and cultured in the presence of PMA/ionomycin/monensin for 5 h. The frequency of GM-CSF-/IL-17A-/IFN-γ-producing cells were analyzed by intracellular staining. Statistical analysis was performed with Student's *t*-test: $^{**}P < 0.01$; $^{***}P < 0.001$; $^{****}P < 0.0001$; n. s. not significant (error bars, SD). Data are representative of 2–6 independent experiments.

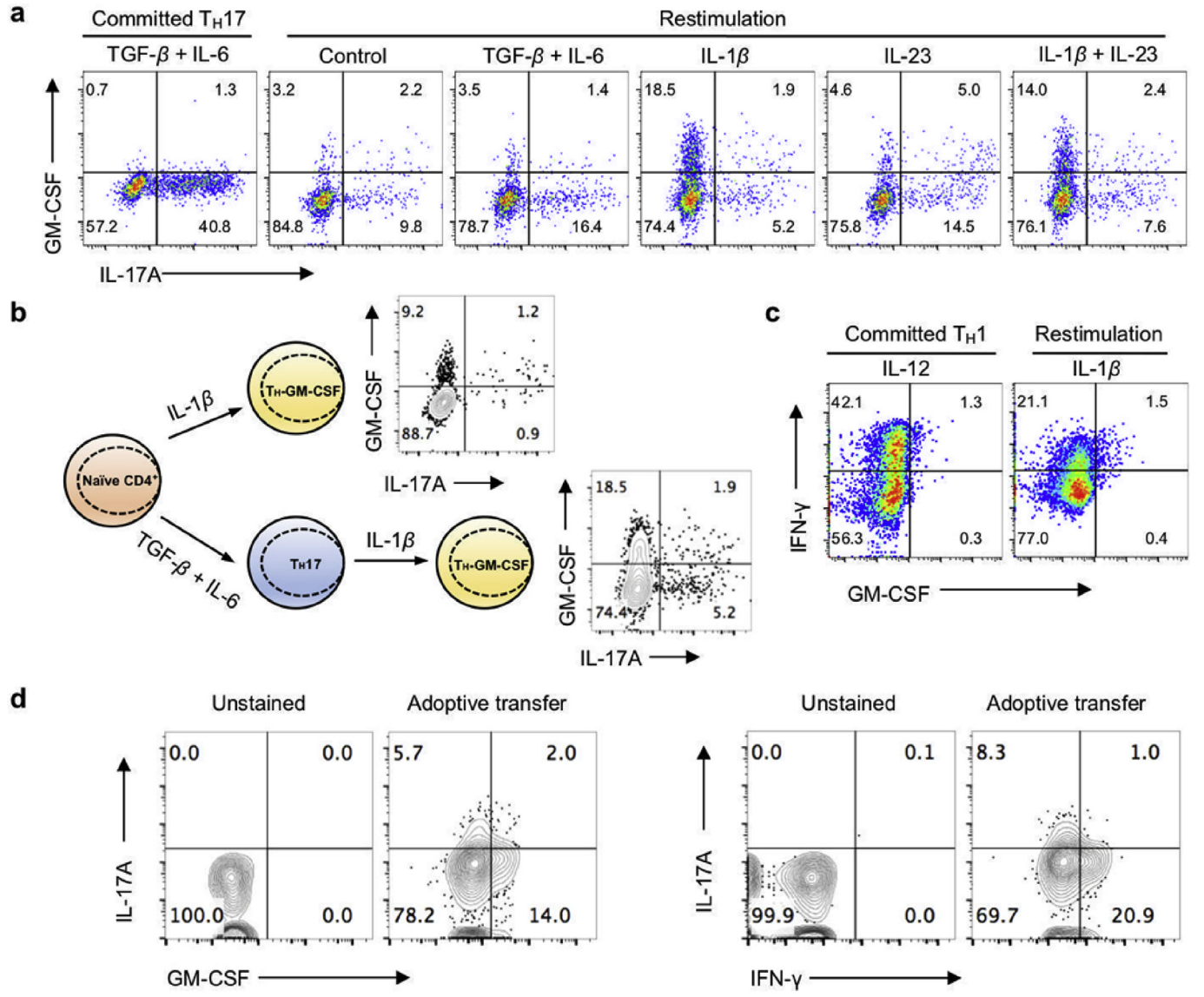

Fig. 2. T_H17 cells possess plasticity to convert into T_H-GM-CSF phenotype. (a) Naïve CD4$^+$ T cells from the spleen and lymph nodes of C57BL/6 mice were differentiated *in vitro* for 3 days under T_H17 polarizing condition. The culture supernatants were then removed and cells were re-cultured with IL-2 without anti-CD3 and anti-CD28 antibodies for 2 days. Cells were then restimulated for 3 days with anti-CD3 and anti-CD28 antibodies in the presence of TGF-β plus IL-6, or IL-1β, or IL-23, or IL-1β plus IL-23, followed by stimulation with PMA/ionomycin/monensin for 5 h and intracellular staining for GM-CSF and IL-17A, and were analyzed by flow cytometry. (b) T_H-GM-CSF cells were differentiated from naïve CD4$^+$ T cells or committed T_H17 cells. (c) Naïve CD4$^+$ T cells from the spleen and lymph nodes of C57BL/6 mice were differentiated *in vitro* for 3 days under T_H1 polarizing condition. The culture supernatants were then removed and cells were re-cultured with IL-2 without anti-CD3 and anti-CD28 antibodies for 2 days. Cells were then restimulated for 3 days with anti-CD3 and anti-CD28 antibodies in the presence of IL-1β, followed by stimulation with PMA/ionomycin/monensin for 5 h and intracellular staining for GM-CSF and IFN-γ, and were analyzed by flow cytometry. (d) Splenic naïve CD4$^+$ T cells from IL-17-GFP reporter mice (CD4$^+$CD44^{lo}CD62L^{hi}eGFP-cells) were differentiated *in vitro* for 3 days under T_H17 polarizing condition. Cells were then sorted by FACS to obtain GFP$^+$ (IL-17-producing) cells and 5×10^5 GFP$^+$ cells were injected (i.p.) into recipient *Rag1*$^{-/-}$ mice. Mice were sacrificed 2 weeks later and CD4$^+$ T cell populations in spleen were analyzed. Data are representative of 2–4 independent experiments.

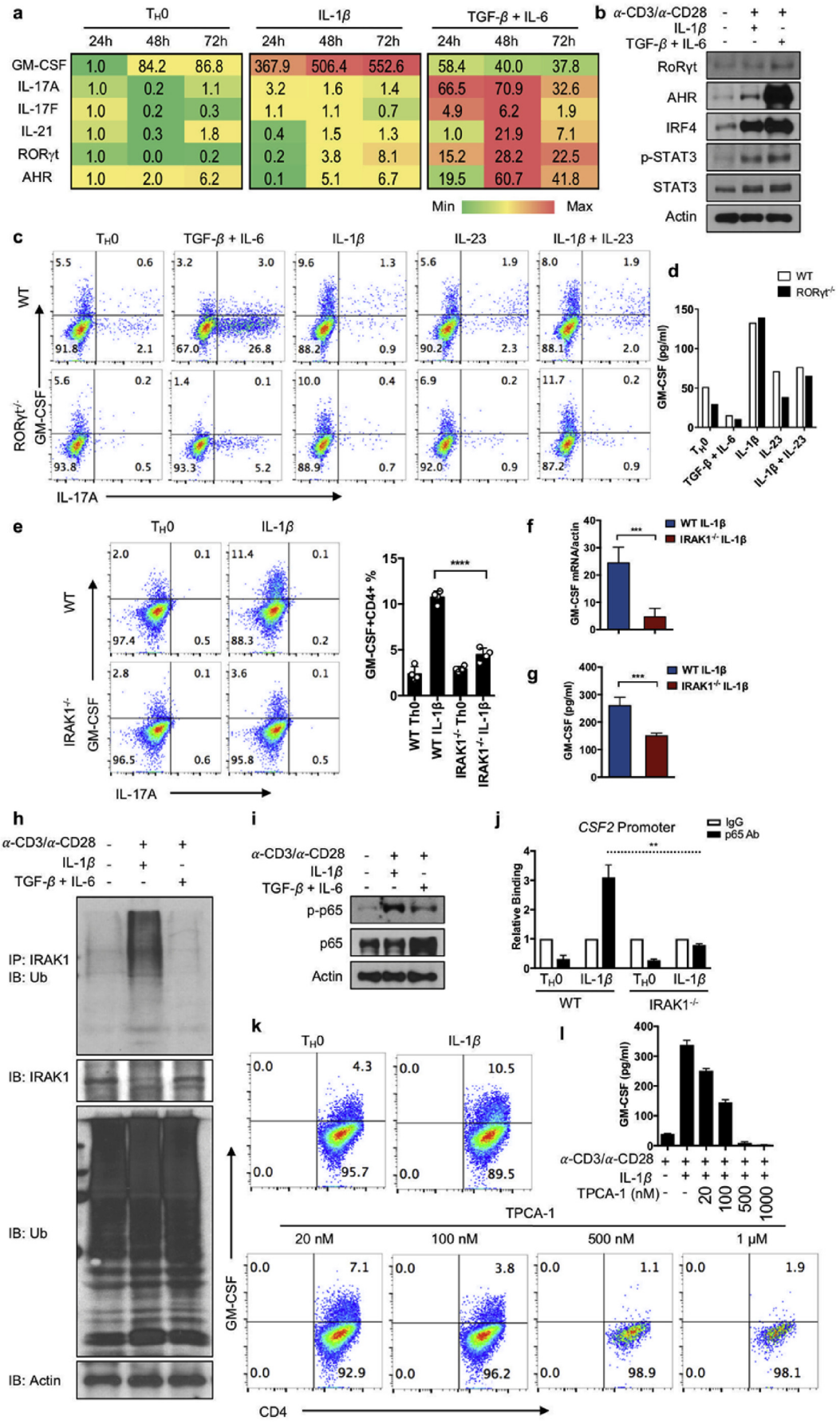

(caption on next page)

Fig. 3. IRAK1-NF-κB axis is required for the generation of T_H-GM-CSF cells. (a) Total RNA from T_H0, T_H-GM-CSF and T_H17 cells was extracted at indicated time points and was analyzed for expression of T_H17 signature genes and GM-CSF by real time RT-PCR. (b) Cellular protein from naïve $CD4^+$ T cells, T_H-GM-CSF and T_H17 cells was subjected to Western blot for detection of T_H17-associated transcription factors. (c) Naïve $CD4^+$ T cells from the spleen and lymph nodes of WT and *RORγt*$^{-/-}$ mice were differentiated *in vitro* for 3 days under T_H0 polarizing conditions or in the presence of TGF-β plus IL-6, or IL-1β, or IL-23, or IL-1β plus IL-23. Cells were then restimulated with PMA/ionomycin/monensin for 5 h, stained for intracellular GM-CSF and IL17A and analyzed by flow cytometry. (d) Supernatants of cells prepared in (c) were analyzed for GM-CSF by ELISA. (e) Naïve $CD4^+$ T cells from the spleen and lymph nodes of WT and *IRAK1*$^{-/-}$ mice were differentiated *in vitro* for 3 days under T_H0 and T_H-GM-CSF polarizing conditions. Cells were then restimulated with PMA/ionomycin/monensin for 5 h, stained for intracellular GM-CSF and IL-17A and analyzed by flow cytometry (left: representative dot plot, right: means of 4 independent experiments). (f) Total RNA from T_H0 and T_H-GM-CSF cells was extracted at 48 h and was analyzed for expression of GM-CSF by real time RT-PCR. (g) Supernatants of cells prepared in (e) were analyzed for GM-CSF by ELISA. (h) Cell lysates from naïve $CD4^+$ T cells, T_H-GM-CSF and T_H17 cells were immunoprecipitated with an anti-IRAK1 antibody and immunoblotted with an anti-ubiquitin antibody. (i) Cellular protein from (h) was subjected to Western blot for detection of the expression and phosphorylation of p65. (j) Naïve $CD4^+$ T cells from WT and *IRAK1*$^{-/-}$ mice were activated for 60 h with anti-CD3 and anti-CD28 antibodies with or without the presence of IL-1β, cells were then subjected to ChIP assay. Three micrograms of an anti-p65 antibody or isotype-matched IgG as control antibody were used in the immunoprecipitation step. PCR was used to quantify the amount of precipitated DNA with primers flanking the p65-binding site of the GM-CSF promoter region. (k) Naïve $CD4^+$ T cells from the spleen and lymph nodes of WT mice were differentiated *in vitro* for 3 days under T_H0 polarizing condition, or in the presence of IL-1β with or without TPCA-1 (0, 20, 100, 500, 1000 nM). GM-CSF expression in each condition was analyzed by intracellular staining. (l) Supernatants of cells prepared in (k) were analyzed by ELISA. Statistical analysis was performed with Student's *t*-test: $^{**}P < 0.01$; $^{***}P < 0.001$; $^{****}P < 0.0001$ (error bars, SD).

ability to convert into T_H-GM-CSF cells *in vivo*.

2.3. IRAK1-NF-κB axis and not RORγt drives T cell GM-CSF production

In an effort to further distinguish $CD4^+$ GM-CSF producing cells from classical T_H17 cells, we examined expression levels of T_H17 signature genes by real-time RT-PCR, and transcription factor expression patterns by immunoblot (Fig. 3a and b). Whereas *in vitro* induced T_H17 cells expressed RORγt [25], aryl hydrocarbon receptor (AHR) [26], and interferon regulatory factor 4 (IRF4) [27], IL-1β-induced T_H-GM-CSF cells expressed significantly lower quantities each of these transcription factors (Fig. 3b and Supplementary Fig. 3a). Furthermore, when we differentiated WT and RORγt-deficient and IL-17-deficient naïve $CD4^+$ T cells with IL-1β *in vitro*, we observed equivalent production of GM-CSF-producing cells in each case (Fig. 3c and d and Supplementary Figs. 3b and c), together demonstrating that neither RORγt nor IL-17 are required for GM-CSF production by T cells.

We next explored the transcriptional regulation underlying T cell production of GM-CSF by IL-1β. As interleukin-1 receptor-associated kinases 1 (IRAK1) is a crucial downstream intermediary of IL-1 signaling and is linked to the transcription factor NF-kappaB (NF-κB) [28], we tested whether IRAK1 is required for IL-1β induced T cell GM-CSF production. When we cultured WT and *IRAK1*$^{-/-}$ naïve $CD4^+$ T cells *in vitro* for three days in the presence of IL-1β, we observed that IRAK1 deficiency dramatically reduced differentiation of $GM\text{-}CSF^+CD4^+$ cells as assessed by flow cytometry (Fig. 3e), and decreased GM-CSF mRNA and GM-CSF secretion into culture supernatants (Fig. 3f and g). In contrast, deficiency of IRAK-M, another member of IRAK family that negatively regulates IL-1 signaling [29], has no impact on IL-1β induced GM-CSF production (Supplementary Figs. 4a and b).

To test for mechanistic links among IL-1β, IRAK1, NF-κB and GM-CSF production, we cultured WT naïve $CD4^+$ T cells with IL-1β or TGF-β/IL-6 for 48 h, and analyzed IRAK1 and the phospho NF-κB p65 by immunoblot. These analyses showed considerably less IRAK1 with significantly more phosphorylation of p65 in the cells stimulated with IL-1β (Fig. 3h and i and Supplementary Figs. 5a and b). To further examine this signaling pathway, the cell lysates were prepared from parallel cultures, were immunoprecipitated with an anti-IRAK1 antibody, and immunoblotted with an anti-ubiquitin antibody (Fig. 3h). These assays showed stimulation with IL-1β induced ubiquitination of IRAK1, which would initiate IL-1/IRAK1 signaling and lead to the downstream activation of p65. We next performed chromatin immunoprecipitation (ChIP) assay and found direct binding of p65 to the promoter region of *CSF2* gene in cells stimulated with IL-1β (Fig. 3j). This binding activity was abrogated in *IRAK1*$^{-/-}$ cells cultured under the same conditions (Fig. 3j). To further test whether NF-κB is required for GM-CSF production by T helper cells, we cultured naïve WT $CD4^+$ T cells with IL-1β plus 2-[(aminocarbonyl)amino]-5-(4-fluorophenyl)-3-thiophenecarboxamide (TPCA-1), an inhibitor of IκB kinase beta (IKKβ) which blocks the NF-κB signaling pathway [30]. These assays showed that both the percentage of $GM\text{-}CSF^+CD4^+$ cells and GM-CSF secretion into culture supernatants were reduced in a dose dependent manner (Fig. 3k,l). TPCA-1 had no effect on T cell apoptosis (Supplementary Fig. 5c), indicating that the reduction was not due to differences in cell death. Taken together, these data establish an essential role for IRAK1/NF-κB in the regulation of GM-CSF production by $CD4^+$ T cells.

Since previous work suggested that STAT4 controls GM-CSF production by both T_H1 and T_H17 cells during EAE [13], we tested whether STAT4 is required for IL-1β-induced T cell production of GM-CSF. Immunoblots showed more STAT4 in IL-1β stimulated cultures compared to IL-6/TGF-β stimulated cells or unstimulated cells (Supplementary Fig. 6a) and *STAT4*$^{-/-}$ prevented IL-1β induced GM-CSF production (Supplementary Fig. 6b). To further characterize the T_H-GM-CSF cell lineage, we performed RNA sequencing analysis to examine gene expression profiles. Analysis of positively regulated genes showed significant enrichment for infectious and immune diseases (Supplementary Figs. 6c–e).

2.4. GM-CSF is not required for T_H17 differentiation

The expression of GM-CSF correlates with the functional maturation of T_H17 cells, and this renders them pathogenic. To determine if intrinsic GM-CSF production is required for the differentiation of T_H17 and other T helper subsets, we activated naïve $CD4^+$ T cells from the spleen and lymph nodes of WT and GM-CSF-deficient (*CSF2*$^{-/-}$) mice *in vitro* for three days under T_H1, T_H2, T_H17, or Treg polarizing conditions and found comparable quantities of these cells in WT and *CSF2*$^{-/-}$ mice (Fig. 4a). Analysis of T_H1 and T_H17 signature genes and supernatants from T_H1 and T_H17 cells confirmed those results (Fig. 4b and c). We then examined T_H1 and T_H17-associated transcript factors including STAT1, STAT4 and RORγt, AHR, IRF4 and STAT3, and the results showed that the transcriptional regulation for T_H1 and T_H17 cells was not affected by GM-CSF deficiency (Fig. 4d and e). In addition, the findings of normally populated $CD4^+$ and $CD8^+$ T cells from *CSF2*$^{-/-}$ mice (Supplementary Fig. 7) eliminated the possibility that GM-CSF deficiency may lead to an abnormal T cell development. These results indicate that steady-state T helper cell development is not intrinsically dependent on GM-CSF production.

2.5. T_H-GM-CSF cells contribute to the development of colitis

To investigate the physiological and pathological function of T_H-GM-CSF in distinct disease models, we adoptively transferred $CD4^+CD45Rb^{hi}$ cells from WT and *CSF2*$^{-/-}$ mice into *Rag1*$^{-/-}$ recipients in an effort to induce colitis. We observed that *Rag1*$^{-/-}$ mice reconstituted with *CSF2*$^{-/-}$ T cells began losing weight later and lost

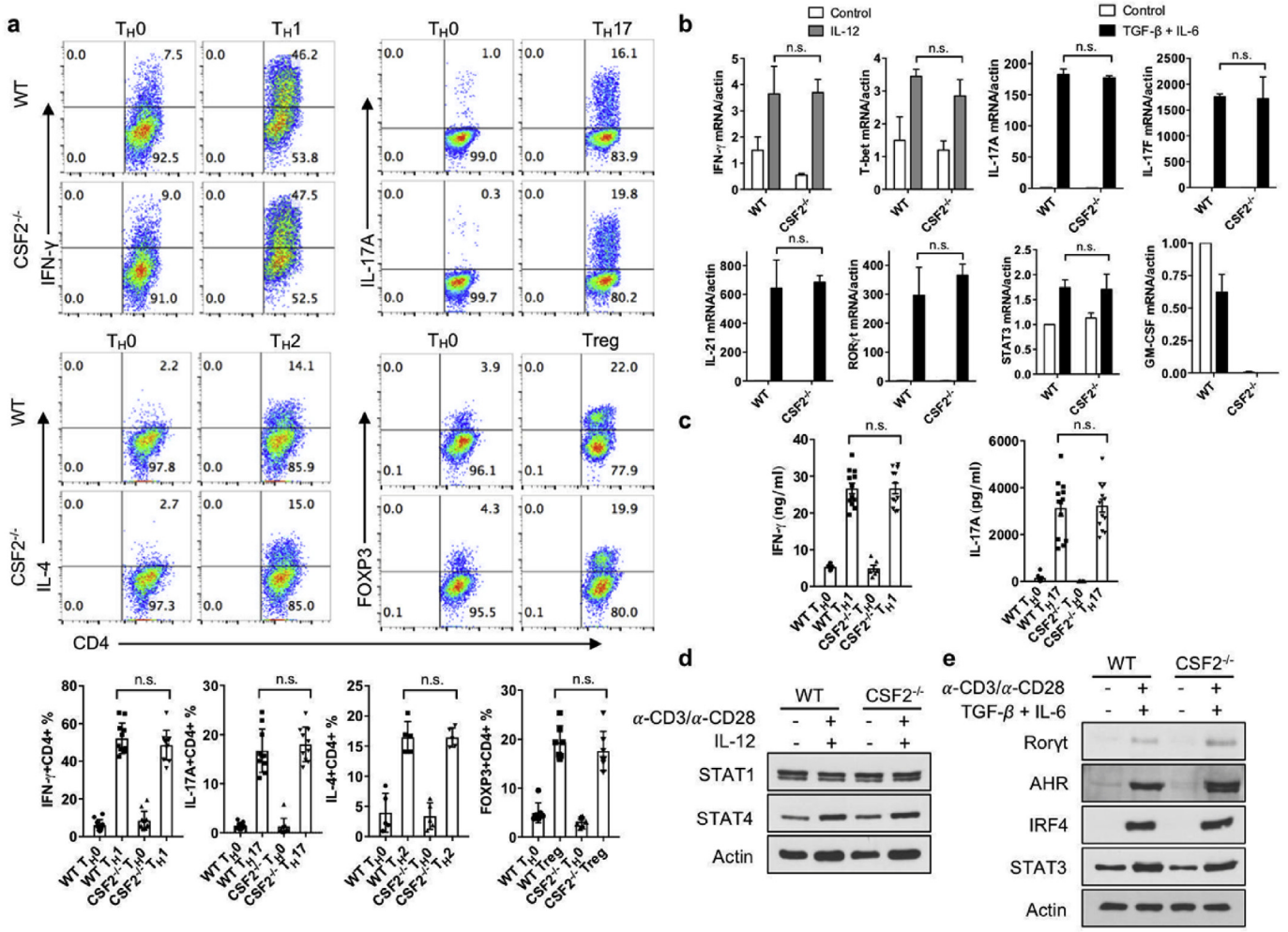

Fig. 4. T helper cell differentiation in *CSF2*$^{-/-}$ CD4^{+} T cells. (a) Naïve CD4^{+} T cells from WT and *CSF2*$^{-/-}$ mice were differentiated *in vitro* for 3 days under T_H1, T_H2, T_H17 or Treg polarizing conditions. Cells were then restimulated with PMA/ionomycin/monensin for 5 h and stained for intracellular IFN-γ, IL-4, IL-17 or Foxp3 and analyzed by flow cytometry (top: representative dot plot, bottom: means of more than 10 independent experiments for T_H1 and T_H17 cells, or more than 5 independent experiments for T_H2 and Treg cells). (b) Total RNA from T_H0, T_H1 and T_H17 cells was extracted at 48 h and was analyzed for expression of T_H1 and T_H17 signature genes by real time RT-PCR. (c) Supernatant from T_H1 or T_H17 cells was analyzed for IFN-γ or IL-17A by ELISA. (d) (e) Cellular protein from T_H1 and T_H17 cells was subjected to Western blot for detection of T_H1- and T_H17-associated transcription factors. Statistical analysis was performed with Student's *t*-test: n. s. not significant (error bars, SD).

significantly less weight than mice adoptively transferred with WT T cells (Fig. 5a). Parallel morphology of the intestines and histologic studies of colonic sections from *Rag1*$^{-/-}$ mice reconstituted with *CSF2*$^{-/-}$ T cells revealed less inflammatory cell infiltrates and significantly lower pathologic scores than those observed in sections from *Rag1*$^{-/-}$ mice reconstituted with WT T cells (Fig. 5b–d). While we detected high frequencies of GM-CSF^{+}CD4^{+} T cells in the colonic lamina propria leukocytes (LPLs) and mesenteric lymph nodes (MLNs) of *Rag1*$^{-/-}$ mice adoptively transferred with WT T cells, no GM-CSF was detected in the *Rag1*$^{-/-}$ mice reconstituted with *CSF2*$^{-/-}$ T (Fig. 5e and f). We observed comparable carboxyfluorescein succinimidyl ester (CFSE) dilution in WT and *CSF2*$^{-/-}$ T cells after activation with anti-CD3 and anti-CD28 antibodies (Fig. 5g), suggesting that the reduced intestinal infiltration was not due to impaired cell proliferation. Control analyses showed that *Rag1*$^{-/-}$ mice transferred with WT or *CSF2*$^{-/-}$ T cells contained comparable percentages of IL-17A- and IFN-γ-producing CD4^{+} T cells in colons (Fig. 5e and f). Previous findings from others [31] and our lab showed that adoptive transfer of *IL-17A*$^{-/-}$ T cells failed to block colitis but instead exacerbated disease progression (data not shown). These results support with previous findings demonstrating that GM-CSF is a key mediator that promotes chronic colitis by skewing hematopoiesis toward granulo-monocytopoiesis and GM-CSF blockade inhibits chronic colitis [32,33]. Thus, our data support the conclusion that GM-CSF-producing T helper cells participate in the pathologenesis of colitis in the system. To verify a detrimental effect of GM-CSF in a separate model of colitis, we induced chronic colitis with low dose of oral DSS (Supplementary Fig. 8a). Disease activity index (DAI) and histopathological features showed that GM-CSF deficiency significantly reduced the clinical and histological expression of disease (Supplementary Figs. 8b–f).

2.6. IL-1 signaling drives colitis by promoting T_H-GM-CSF accumulation

Our above data showed that *in vitro* T_H-GM-CSF differentiation is IL-1β dependent. To address whether IL-1 signaling is also required for promoting T cell GM-CSF production in the context of inflammation, we transferred naïve CD4^{+}CD45Rb^{hi} cells from WT or *IL1R1*$^{-/-}$ mice into *Rag1*$^{-/-}$ recipients to induce colitis and assessed the development of pathology. While adoptively transferred WT cells induced an expected weight loss with severe inflammation in (Fig. 6a–e), transfer of naïve *IL1R1*$^{-/-}$ CD4^{+} T cells caused significantly less weight loss with less severe intestinal inflammation (Fig. 6a–e). Despite this attenuated intestinal inflammation, we did not observe significant differences in the proportions of IL-17A- and IFN-γ-producing CD4^{+} T cells in *Rag1*$^{-/-}$

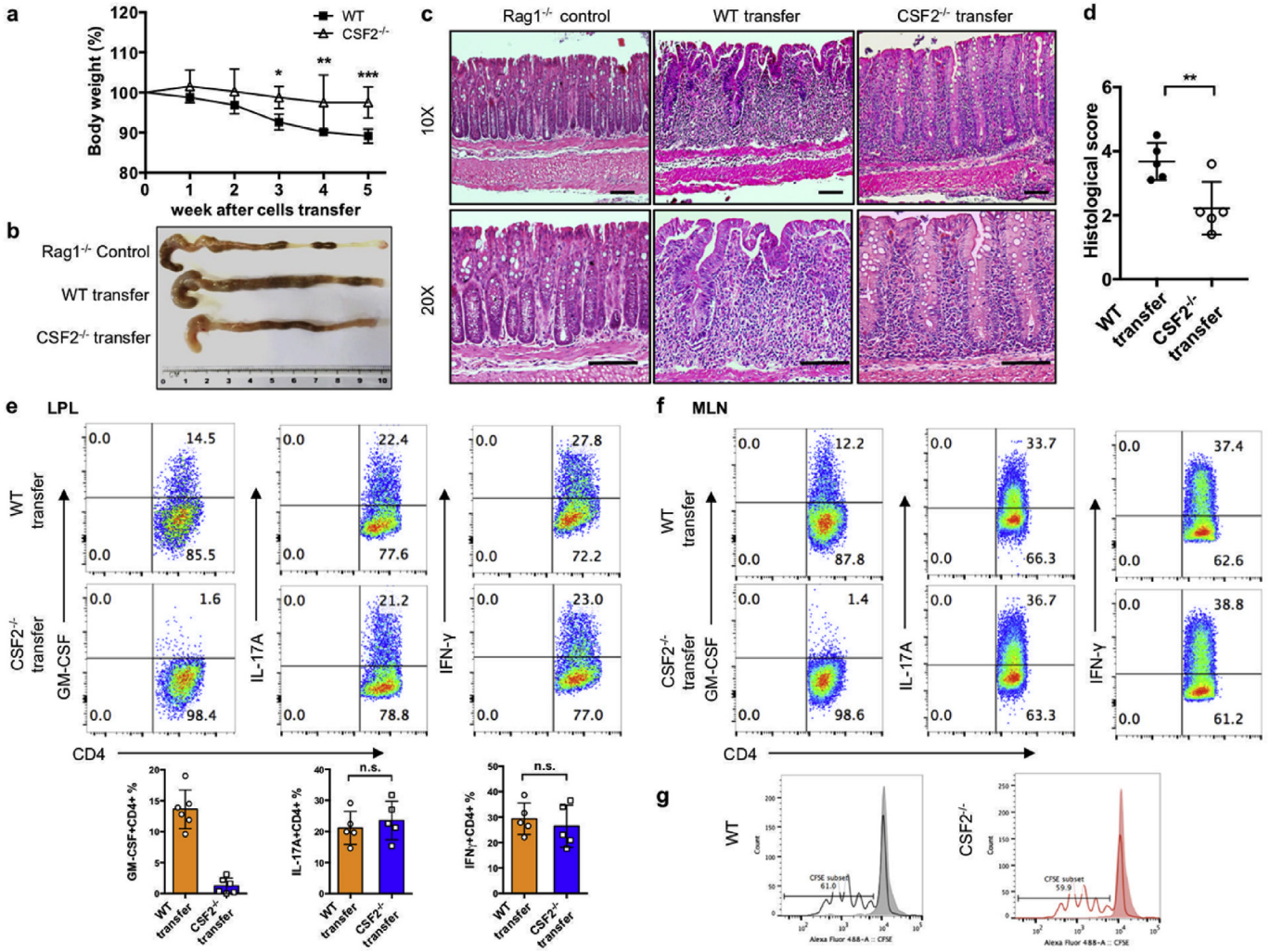

Fig. 5. T cell-derived GM-CSF contributes to the development of colitis. $CD4^+CD45RB^{hi}$ T cells were purified from spleen and lymph nodes of WT and *CSF2*$^{-/-}$ mice and 5×10^5 cells were injected (i.p.) into recipient *Rag1*$^{-/-}$ mice. Body weight change was monitored every week and mice were sacrificed 5 weeks later. (a) Changes in body weight of *Rag1*$^{-/-}$ mice after transfer of WT and *CSF2*$^{-/-}$ T cells. (b) Gross morphology of colons. (c) Sections of colons from *Rag1*$^{-/-}$ mice (*Rag1*$^{-/-}$ control) or *Rag1*$^{-/-}$ mice transferred with $CD4^+CD45RB^{hi}$ T cells from WT mice (WT transfer) or *CSF2*$^{-/-}$ mice (*CSF2*$^{-/-}$ transfer). Scale bars, upper panel, 100 μm; low panel, 50 μm. (d) Histological scores of the colons of *Rag1*$^{-/-}$ mice transferred with WT or *CSF2*$^{-/-}$ T cells. (e) Colonic lamina propria leukocytes (LPLs) of *Rag1*$^{-/-}$ mice transferred with WT or *CSF2*$^{-/-}$ T cells were isolated and cultured in the presence of PMA/ionomycin/monensin for 5 h. Frequency of indicated $CD4^+$ T cell populations were analyzed by flow cytometry (top: representative dot plot, bottom: means, n = 4 from 2 independent experiments). (f) MLNs of *Rag1*$^{-/-}$ mice transferred with WT or *CSF2*$^{-/-}$ T cells were isolated and cells were cultured in the presence of PMA/ionomycin/monensin for 5 h. Frequency of indicated $CD4^+$ T cell populations were analyzed by flow cytometry. (g) WT and *CSF2*$^{-/-}$ $CD4^+$ T cells from the spleens and lymph nodes were labeled with CFSE. T cell proliferation was analyzed. Statistical analysis was performed with Student's *t*-test: $*P < 0.05$; $**P < 0.01$; $***P < 0.001$ (error bars, SD). Data are representative of 2 independent experiments.

mice receiving WT or *IL1R1*$^{-/-}$ naïve $CD4^+$ cells (Fig. 6f and g). In contrast, *Rag1*$^{-/-}$ recipients with adoptively transferred *IL1R1*$^{-/-}$ naïve $CD4^+$ T cells exhibited a considerably decreased percentage of $GM\text{-}CSF^+CD4^+$ cells when compared with recipients of WT naïve $CD4^+$ T cells (Fig. 6f and g). Together with the above *in vitro* data the findings indicate that IL-1 signaling is essential for promoting T_H-GM-CSF accumulation in the colon, and thereby drives the pathogenesis of T cell mediated colitis.

2.7. T cell GM-CSF activates macrophages

Although activated T cells are considered the primary triggers of immune responses, myeloid cells are equipped to cause tissue damage in most autoimmune and inflammatory diseases [3]. To investigate the relative contribution of myeloid compartment downstream of GM-CSF, we performed immunofluorescence staining of colon tissue from the above experiments. These experiments revealed reduced $F4/80^+$ cell infiltrates in *Rag1*$^{-/-}$ deficient recipients of *CSF2*$^{-/-}$ vs WT T cells (Fig. 7a). The absence of *CSF2* from the adoptively transferred T cells only modestly altered staining for $Gr\text{-}1^+$ cells (Fig. 7a), suggesting that macrophages are main effector cells for GM-CSF. In further support of this conclusion, we observed significantly less mRNA for classically activated macrophage (M1) [34] signature genes, including IL-12 p40, NOS2, TNF-α, IL-6 and interferon regulatory factor 5 (IRF5) [35], in the colon of *Rag1*$^{-/-}$ mice reconstituted with *CSF2*$^{-/-}$ T cells compared to WT transfer controls (Fig. 7b). These results suggest that T cell produced GM-CSF-regulates colonic M1 macrophage activation, contributing to the development of colitis.

To provide further insight into mechanisms through which GM-CSF regulates M1 macrophage differentiation, we harvested peritoneal macrophages from WT and *CSF2*$^{-/-}$ mice and activated them *in vitro* with LPS plus IFN-γ. These assays showed that the percentage of iNOS- and IL-12 p40-expressing cells was significantly reduced in *CSF2*$^{-/-}$ mice when compared to WT controls (Fig. 8a). Likewise, the expression

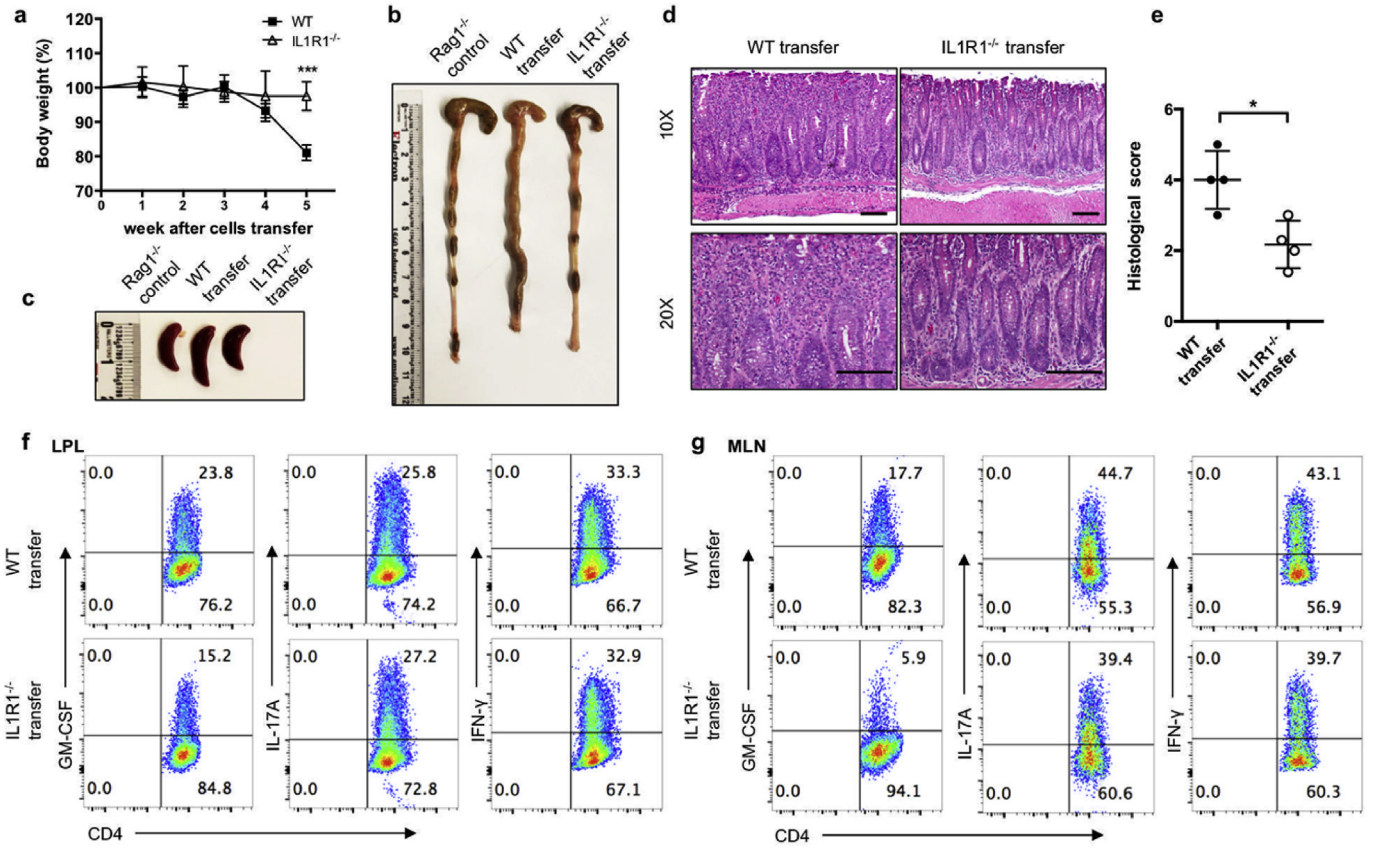

Fig. 6. IL-1 signaling is required for T_H-GM-CSF accumulation in colitis. $CD4^+$ $CD45RB^{hi}$ T cells were purified from spleen and lymph nodes of WT and *IL1R1*$^{-/-}$ mice and 5×10^5 cells were injected (i.p.) into recipient *Rag1*$^{-/-}$ mice. Body weight change was monitored every week and mice were sacrificed 5 weeks later. (a) Changes in body weight of *Rag1*$^{-/-}$ mice after transfer of WT and *IL1R1*$^{-/-}$ T cells. (b) Gross morphology of colons. (c) Gross morphology of spleens. (d) Sections of colons from *Rag1*$^{-/-}$ mice transferred with $CD4^+CD45RB^{hi}$ T cells from WT mice (WT transfer) or *IL1R1*$^{-/-}$ mice (*IL1R1*$^{-/-}$ transfer). Scale bars, upper panel, 100 μm; low panel, 50 μm. (e) Histological scores of the colons of *Rag1*$^{-/-}$ mice transferred with WT or *IL1R1*$^{-/-}$ T cells. (f) LPLs of *Rag1*$^{-/-}$ mice transferred with WT or *IL1R1*$^{-/-}$ T cells were isolated and cultured in the presence of PMA/ionomycin/monensin for 5 h. Frequency of indicated $CD4^+$ T cell populations were analyzed by flow cytometry. (g) MLNs of *Rag1*$^{-/-}$ mice transferred with WT or *IL1R1*$^{-/-}$ T cells were isolated and cells were cultured in the presence of PMA/ionomycin/monensin for 5 h. Frequency of indicated $CD4^+$ T cell populations were analyzed by flow cytometry. Statistical analysis was performed with Student's *t*-test: $*P < 0.05$; $**P < 0.01$; $***P < 0.001$ (error bars, SD). Data are representative of 2 independent experiments.

of NOS2 and IRF5 was downregulated at protein level by the depletion of GM-CSF (Fig. 8b). Analysis of NO, IL-12p40 and IL-6 secretion into the supernatants of WT and *CSF2*$^{-/-}$ M1 macrophages, and analysis of mRNA expression of M1 signature genes confirmed these results (Fig. 8c and d). Although we (Supplementary Fig. 9) and others [3] demonstrated that the development of myeloid cells was not perturbed by GM-CSF deficiency, we challenged WT and *CSF2*$^{-/-}$ mice with an intraperitoneal injection of LPS and found that all LPS-treated WT mice initially appeared more lethargic and eventually exhibited other manifestations of illness prior to death when compared to LPS-treated *CSF2*$^{-/-}$ mice (Fig. 8e). The production of M1-associated molecules in the sera and the mRNA expression of M1 signature genes were clearly reduced in *CSF2*$^{-/-}$ mice after LPS injection (Fig. 8f and g), whereas M2-related genes such as IL-10 and Arg-1 [34] were upregulated (Fig. 8f). These results demonstrate that GM-CSF is essential for *in vivo* M1 macrophage activation.

3. Discussion

Naïve $CD4^+$ T cells clonally expand and differentiate into a variety of effector subsets after encountering specific antigens, acquiring the ability to direct diverse immune responses, where they serve either protective roles by combating exogenous pathogens or function as deleterious factors by being self-reactive. The distinctive differentiation programs are largely influenced by the milieu of microenvironmental cytokines. As well-established, IL-12 drives polarization of T_H1 cells and IL-4 drives polarization of T_H2 cells [24]. After longstanding investigations on T_H1/T_H2 paradigm, the identification of T_H17 cells widened the framework of T helper cell lineages and complicated the patterns of cytokines and transcript factors responsible for the lineage decisions. While TGF-β and IL-6 induce the initial T_H17 development, IL-23 is required for the terminal differentiation and full function of T_H17 cells during immune responses [36]. It was not until GM-CSF was identified as one of the IL-23-induced factors did it become clear that GM-CSF, rather than any other T_H17 cytokines features the pathogenicity of both activated T_H17 cells and autoreactive T helper cells in the context of inflammation [9,10,13]. Although the distinction between GM-CSF-expressing pathogenic T_H17 cells and GM-CSF-producing $CD4^+$ T cells that emerge during T_H17 immunity has been largely blurred due to their overlapping contribution to immune pathogenesis, the population of GM-CSF-producing $CD4^+$ T cells that lack IL-17 and IFN-γ expression is indeed present and cannot be disregarded.

Herein, we provide *in vitro* and *in vivo* evidence that GM-CSF-producing $CD4^+$ T cells are a unique T helper subset, which we designated as T_H-GM-CSF. Instead of IL-23, the prototypic proinflammatory cytokine IL-1β directly programs GM-CSF production independent of RORγt. Compared with IL-1β alone, the combination of IL-1β and IL-23 did not result in a higher proportion of GM-CSF-producing $CD4^+$ T cells, which confirmed a prominent role of IL-1β, but in contrast a redundant role of IL-23 in the cell differentiation. We also found that

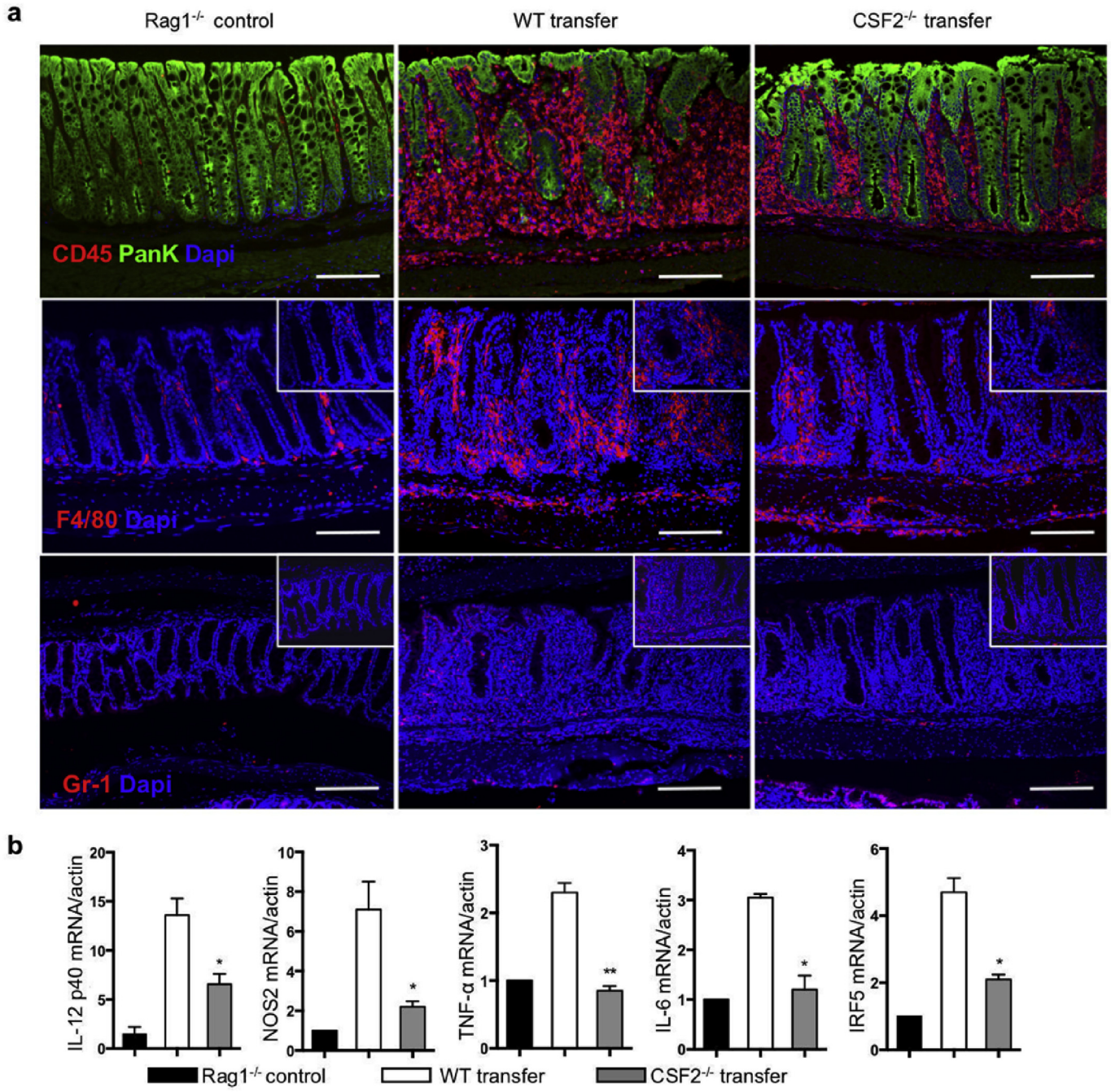

Fig. 7. GM-CSF deficiency ameliorates colitis with reduced infiltration and activation of macrophages. (a) Immunostaining of CD45, Pan-keratin, F4/80 and Gr-1 in the intestine of *Rag1*$^{-/-}$ mice (*Rag1*$^{-/-}$ control) or *Rag1*$^{-/-}$ mice transferred with CD4^{+}CD45RB^{hi} T cells from WT mice (WT transfer) or *CSF2*$^{-/-}$ mice (*CSF2*$^{-/-}$ transfer). Scale bars, 100 μm. (b) The mRNA expression of M1 macrophage signature genes in mice described in (a) was analyzed by real time RT-PCR. Statistical analysis was performed with Student's *t*-test $^{*}P < 0.05$; $^{**}P < 0.01$ (error bars, SD). Data are representative of 2 independent experiments.

while other T helper cells including T_H1, T_H2, Treg and T_{FH} produced equally small amounts of GM-CSF, TGF-β/IL-6 conditioned T_H17 had lower levels of GM-CSF production. These findings coincide with a previous study showing that IL-17 and GM-CSF expression are regulated in a reciprocal manner in human T helper cells [16]. This also verified our hypothesis that GM-CSF-producing CD4^{+} T cells are distinct from T_H17 and other previously identified T helper cells. Our identification of T_H-GM-CSF provides an alternative explanation for the pathogenesis of certain inflammatory and autoimmune diseases, where the desired therapeutic effect cannot be achieved by the blockade of the key components of T_H1 and T_H17 cells [37,38].

Both *in vitro* and *in vivo* studies have shown that T cell differentiation is a reversible and flexible process, in which the committed T cells can acquire the features of mixed or alternative effector fates upon changing circumstances [21–23,39]. A good example is T_H17, the cells with high plasticity, may shift their phenotype towards increased IFN-γ expression and decreased IL-17 expression in the presence of IL-12 and IL-23[21]. Similarly, IL-1β has also been shown to be essential for IFN-γ expression in pathogen-induced human T_H17 cells and this T_H17/T_H1 subset is frequently observed in pathological conditions [23]. Interestingly, by restimulating T_H17 cells with IL-1β alone, we showed that although there was a small fraction of GM-CSF/IL-17A double producing cells, GM-CSF single producing cells accounted for the largest proportion among all tested CD4^{+} T cells. These unclassified

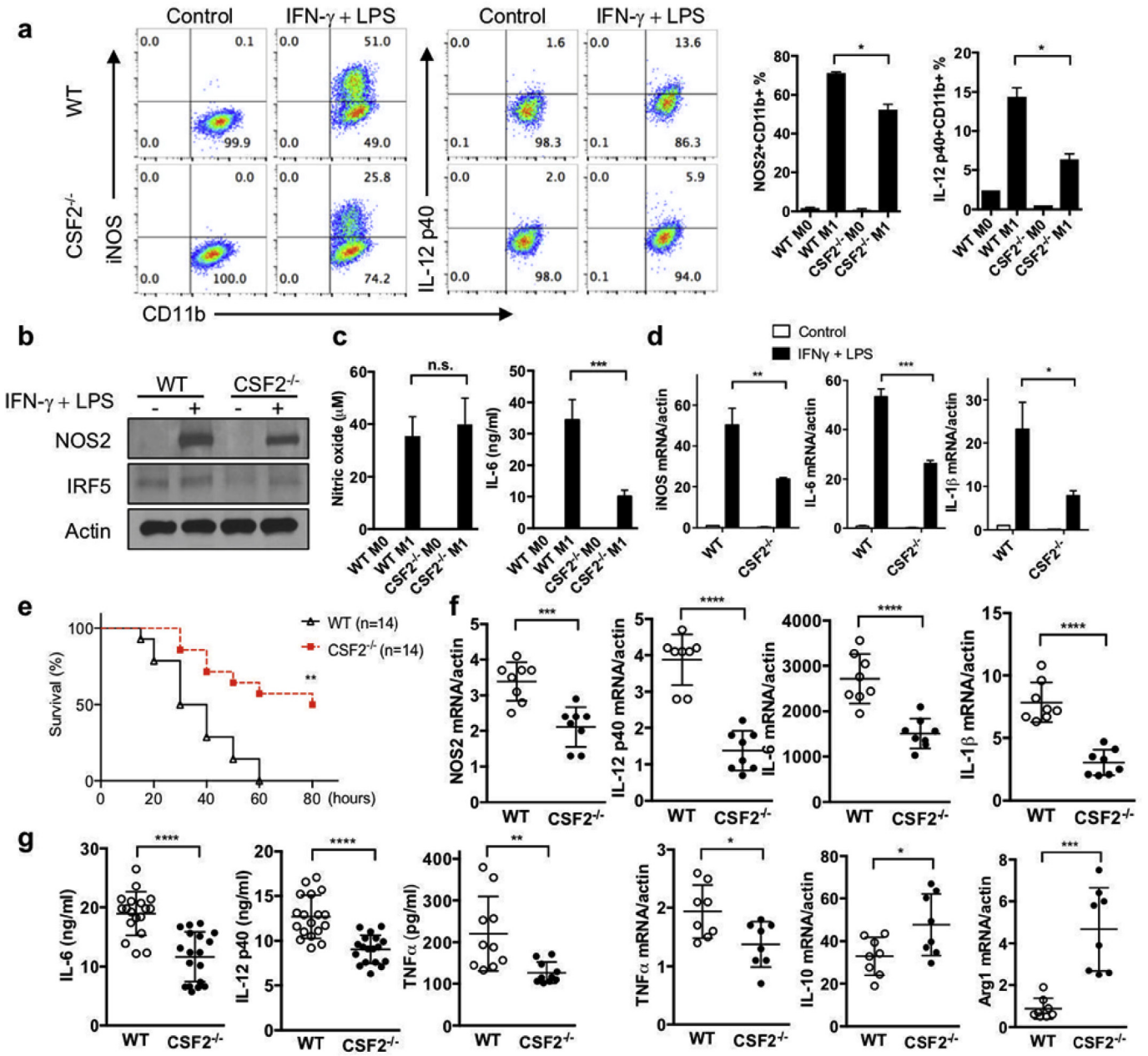

Fig. 8. GM-CSF deficiency impairs M1 macrophage activation *in vitro* and *in vivo*. (a) Peritoneal macrophages from WT and *CSF2*$^{-/-}$ mice were stimulated with IFN-γ (10 ng/ml) plus LPS (200 ng/ml) for 24 h, stained for intracellular iNOS and IL-12 p40 and analyzed by flow cytometry (left: representative dot plot, right: means of 2 independent experiments). (b) Cellular protein from macrophages prepared in (a) was subjected to Western blot for detection of NOS2 and IRF5. (c) Supernatants of cells prepared in (a) were analyzed for nitric oxide (NO) by colorimetric assay and for IL-6 by ELISA. (d) Peritoneal macrophages from WT and *CSF2*$^{-/-}$ mice were stimulated with IFN-γ (10 ng/ml) plus LPS (200 ng/ml) for 6 h and real time RT-PCR was performed for the analysis of M1 macrophage gene expression. (e) WT or *CSF2*$^{-/-}$ mice were injected (i.p.) with LPS (500 ng per mouse). The survival of mice was observed (WT = 14 and *CSF2*$^{-/-}$ = 14 mice from 2 independent experiments). (f) Total tissue RNA was extracted from spleens, and real time RT-PCR was performed for the analysis of mRNA expression of indicated genes. The data are representative of two independent experiments. (g) The sera level of IL-6, IL-12 p40 and TNFα was determined by ELISA. Statistical analysis was performed with Student's *t*-test: $^{*}P < 0.05$; $^{**}P < 0.01$; $^{***}P < 0.001$; $^{****}P < 0.0001$ (error bars, SD).

cells originated from T_H17, but could not be considered GM-CSF-expressing pathogenic T_H17 cells as described previously, because they did not express IL-17A. It seemed likely that in addition to programing the initial differentiation of T_H-GM-CSF from naïve precursors, IL-1β also drove the switch from the T_H17 phenotype to the T_H-GM-CSF phenotype. We could not draw a definitive conclusion as to whether these T_H17-derived T_H-GM-CSF cells are the same as those differentiated directly from naïve CD4$^+$ T cells, as we described above. One indication of this issue is the fact that T_H17-derived T_H1 cells are found in the synovial fluid of patients with juvenile idiopathic arthritis [40,41], and they are known as "non-classic" T_H1 cells, which are clearly different from the "classic" T_H1 cells, based on their respective expression patterns of cell surface maker CD161 and chemokine receptors CCR6 and CXCR3[40, 41]. Nevertheless, these findings regarding the T_H17-to-T_H-GM-CSF shift are intriguing, given that GM-CSF production is responsible for T cell pathogenicity, they indicate that this transition could be a detrimental process during disease cycle. Beyond the involvement of GM-CSF in T_H17 or other T helper cell pathways, GM-CSF-producing CD4$^+$ T cells induced by IL-1β, regardless of their origins, could be involved in immune dysregulation under alternative

circumstances.

There is some controversy as to which transcript factors influence GM-CSF production in T cells. RORγt was thought to be important in inducing expression of GM-CSF in T helper cells, however, we and others [10] have suggested a dispensable role of RORγt in this process, since $CD4^+$ T cells from RORγt-deficient mice retained their ability to produce large amounts of GM-CSF. We found, however, IRAK1-NF-κB axis was pivotal during the development of T_H-GM-CSF cells. IRAK1 is one of the putative serine/threonine kinase that is associated with IL-1 receptor (IL1R) upon IL-1 engagement. IRAK1 is then phosphorylated and ubiquitinated to propagate downstream signals [28,42]. The NF-κB family of transcription factors is a primary group of effectors downstream of IL-1β/IRAK signaling, and they regulate a large profile of genes in nucleus [28,42]. In the present study, we observed that IRAK1 was required for GM-CSF induction, as polarization of $CD4^+$ T cell from *IRAK1*$^{-/-}$ mice in the presence of IL-1β resulted in significantly impaired GM-CSF expression and secretion. We also found that IRAK1 expression was considerably diminished in T_H-GM-CSF cells due to ubiquitination, but not in T_H17 cells or naïve $CD4^+$ T cells. NF-κB p65 was then activated in T_H-GM-CSF cells and it directly bound to the promoter region of *CSF2* gene. However, this binding activity was diminished by IRAK1 deficiency. Finally, blockage of NF-κB pathway reduced GM-CSF production in $CD4^+$ T cells cultured in the presence of IL-1β.

Given that IL-1β is an inducer of GM-CSF, it is reasonable to assume that components of the IL-1β signaling pathway may participate in the regulation of GM-CSF expression. Previous studies have shown that MyD88, the adaptor protein that is recruited after the initiation of IL-1β signaling, is responsible for GM-CSF production in both T cells and innate lymphoid cells (ILCs). Although other transcript factors, such as STAT4 and STAT5[5, 11, 14], have also been described to play an important role in the induction of GM-CSF by T cells, this is the first time IRAK1 has been implicated in the IL-1β-elicited T_H-GM-CSF program, showing that IRAK1- NF-κB axis plays an essential role for the differentiation of these cells. Our future studies will focus on the investigation of transcriptome of T_H-GM-CSF cells and identify the transcriptional network for the regulation of T_H-GM-CSF cell differentiation.

In contrast to the well-established pathogenic features in EAE, GM-CSF seems to play both protective and pathogenic roles in human IBD and mouse colitis [5,32,33,43–46]. Recent publications have demonstrated that T cell-derived GM-CSF is a key mediator in IL-23-driven colitis by dysregulation of upstream hematopoietic cells [32], while others have provided evidence that GM-CSF produced by RORγt$^+$ type 3 innate lymphoid cells (ILC3) exerts beneficial effects on intestinal homeostasis through the maintenance of colonic Treg cells [5]. As such, it is likely that the diverse role of GM-CSF in colitis is due to different cellular sources, temporal production, and the microenvironment in which it is produced.

Classically, both T_H1 and T_H17 cells are known as major mediators that contribute to IBD pathogenesis. However, therapeutic interventions that result in selective depletion of the signature factors of T_H1 and T_H17 cells result in adverse outcomes or are only partial effective [37,38]. By contrast, a central role for GM-CSF produced by effector T helper cells in triggering autoimmune and inflammatory disorders has emerged [9–11,32]. By transferring naïve $CD4^+CD45Rb^{hi}$ T cells from WT mice and *CSF2*$^{-/-}$ mice into *Rag1*$^{-/-}$ mice, we determined that GM-CSF-producing $CD4^+$ T cells participated in the development of colitis independently of the T_H1 and T_H17 pathways. One possible explanation regarding how these GM-CSF-producing $CD4^+$ T cells were generated is that in tissue inflammation, either invading or tissue resident myeloid cells are recruited for infiltration and accumulation, resulting in tissue damage [3,12]. The central role of innate myeloid cells is reflected in the potential proinflammatory effects of the cytokines that they secrete. Cytokines such as IL-23 and IL-1β can induce GM-CSF production in T_H1 and/or T_H17 cells, as described previously, or elicit the differentiation program for GM-CSF single producing $CD4^+$ T cells, as shown in this study. Alternatively, during chronic intestinal inflammation, the features of effector T helper cells are shaped by the local tissue microenvironment. This is seen in T_H17 cells and possibly other T helper cells that may switch from a non-pathogenic phenotype toward a GM-CSF-producing pathogenic phenotype in response to the changing contexts. Thus, T cell-derived GM-CSF that targets myeloid cells contributes to the intestinal inflammation.

It is noticeable that the adoptively restricted loss of GM-CSF by $CD4^+$ T cells did not completely eliminate colitis in GM-CSF-competent mice, this could be due to the involvement of GM-CSF produced by innate immune cells, but also indicated a more ambiguous pathogenesis of colitis and human IBD in which GM-CSF-producing $CD4^+$ T cells as well as other T helper cells and their cytokines would not function alone, but instead, closely collaborate with or have modulating effect on each other.

In summary, our data demonstrate a new concept that IL-1β-elicited GM-CSF-producing $CD4^+$ T cells represent a unique lineage of T helper cells, in which IRAK1-NF-κB axis serves as the primary transcriptional regulator. The distinction between GM-CSF-producing $CD4^+$ T cells from various origins and their ultimate fates, especially under disease conditions, require further investigations. Here, we have shown that GM-CSF production by $CD4^+$ T cells participates in the induction of mouse chronic colitis. Our view on the possibility that synergy between each T helper cell subset and the cytokines they secrete can orchestrate the destination of the disease may provide a better understanding on the complexity of T cell-mediated pathogenesis.

4. Materials and methods

4.1. Mice

Wild-type (C57BL/6J) mice and B6.129S7-Il1r1^{tm1Imx}/J (*IL1R1*$^{-/-}$), B6.129S7-Rag1^{tm1Mom}/J (*Rag1*$^{-/-}$), B6.129P2-Il17a^{tm1Yiw}/J (*IL17A*$^{-/-}$), B6.129P2-Rorc^{tm1Litt}/J (*RORγt*$^{-/-}$), C57BL/6J-Stat4e^{m3Adiuj}/J (*STAT4*$^{-/-}$), and C57BL/6-Il17a^{tm1Bcgen}/J (IL-17-GFP reporter) mice were purchased from The Jackson Laboratory and maintained at the Icahn School of Medicine at Mount Sinai. B6.129S-Csf2^{tm1Mlg}/J (*CSF2*$^{-/-}$) mice were a kind gift from Dr. Arthur Mortha. B6. Cg-Irak1^{tm1Jth}/CpasJ (*IRAK1*$^{-/-}$) mice and B6.129S1-Irak3^{tm1Flv}/J (*IRAK-M*$^{-/-}$) mice were kind gifts from Dr. Yao Zhang. The animal study protocols were approved by the Institutional Animal Care and Use Committees of Mount Sinai School of Medicine.

4.2. Antibodies

The following Flow cytometry antibodies were purchased from BD-Biosciences (USA), and conjugated to FITC, PE, PE-Cy5, PE-Cy7, PerCP-Cy5.5, PerCP-eFluor 710, eFluor 450 or APC: CD45RB (C363.16A), and isotype controls. Antibodies for CD4 (L3T4), CD25 (PC61.5), CD44 (1M7), CD62L (MEL-14), GM-CSF (MP1-22E9), IL-17a (TC11-18H10), IFN-γ (XMG1.2), IL-4 (11B11), FOXP3 (FJK-16S), CD11b (M1/70), Gr-1 (RB6-8C5), NOS2 (CXNFT), and IL-12/IL-23 p40 (C17.8) were purchased from ThermoFisher (eBioscience). FITC Annexin V Apoptosis Detection Kit I (2293683) was purchased from BD Phamingen. Western blot antibodies RORγt (B2D), AHR (polyclonal) and Ubiquitin (Ubi-1) respectively were purchased from ThermoFisher (eBioscience), Abcam and ThermoFisher (Invitrogen); IRF4 (D9P5H), p-STAT3 (Tyr705, D3A7), STAT3 (124H6), β-actin (8H10D10), IRAK1 (D51G7), p-p65 (Ser536, 93H1), p65 (D14E12), STAT1 (D1K9Y), STAT4 (C46B10), NOS2 (D6B6S), IRF5 (Rodent Specific) were purchased from Cell Signaling Technology (CST) and were used according to the manufacturers' instructions. Secondary antibodies were from Santa Cruz Biotechnology, Inc.

4.3. $CD4^+$ T cell preparation and differentiation in vitro

Naive $CD4^+$ T cells ($CD62L^+CD44^{lo}$) were prepared by fluorescence-activated cell sorting (FACS) from the spleens and lymph nodes of WT, *IL1R1*$^{-/-}$, *ROR*$\gamma t^{-/-}$, *IL-17A*$^{-/-}$, *CSF2*$^{-/-}$, *IRAK1*$^{-/-}$, *IRAK-M*$^{-/-}$ *or STAT4*$^{-/-}$ mice. The sorted cells were primed *in vitro* for 72 h with anti-CD3 (2 μg/ml; 145-2C11; BD Biosciences) and anti-CD28 (2 μg/ml; 37.51; BD Biosciences) antibodies. The cells were then restimulated for 5 h with PMA/ionomycin/monensin and intracellular cytokines were measured by flow cytometry. Cells stimulated under neutral conditions were defined as T_H0 cells. Cells were stimulated to differentiate into T_H1 cells by supplementation with IL-12 (25 ng/ml; R &D Systems) plus anti-IL-4 antibody (10 μg/ml; 11B11; BD Bioscences), or into T_H2 cells by supplementation with IL-4 (25 ng/ml; R&D Systems) plus anti-IFN-γ antibody (10 μg/ml; XMG1.2, BD Biosciences), or into T_H17 cells by supplementation with transforming growth factor-β1 (TGF-β; 5 ng/ml) and IL-6 (25 ng/ml; both from R&D Systems) in the presence of anti-IFN-γ antibody (10 μg/ml; XMG1.2, BD Biosciences) and anti-IL-4 antibody (10 μg/ml; 11B11; BD Biosciences), or into Treg cells by supplementation with TGF-β (50 ng/ml; R&D Systems), or into T_{FH} cells by supplementation with IL-21 (25 ng/ml) and IL-6 (10 ng/ml; both from R&D Systems). For T_H-GM-CSF cell differentiation, cells were stimulated by supplementation with IL-1β (20 ng/ml; R&D Systems) in the presence of anti-IFN-γ antibody (10 μg/ml; XMG1.2, BD Biosciences), anti-IL-4 antibody (10 μg/ml; 11B11; BD Biosciences) and anti-TGF-β antibody (10 μg/ml; A75-2; all from BD Biosciences). For 8-day cultured $CD4^+$ T cells, cells were activated *in vitro* for 72 h under T_H17, T_H1, or Treg conditions (1st stimulation), allowed to "rest" for 48 h in the presence of IL-2 (20 ng/ml; R&D Systems), and then re-activated for 72 h with anti-CD3 and anti-CD28 antibodies in the presence of TGF-β (5 ng/ml; R&D Systems) plus IL-6 (25 ng/ml; R&D Systems), or IL-1β (20 ng/ml; R&D Systems) with or without IL-23 (20 ng/ml; R&D Systems) (2nd stimulation).

4.4. Intracellular staining and flow cytometry

For T cells, naïve $CD4^+$ T cells ($CD62L^+CD44^{lo}$) were prepared by FACS from spleens and lymph nodes of WT, *IL1R1*$^{-/-}$, *ROR*$\gamma t^{-/-}$, *IL-17A*$^{-/-}$, *CSF2*$^{-/-}$, *IRAK1*$^{-/-}$, *IRAK-M*$^{-/-}$ *or STAT4*$^{-/-}$ mice. The sorted cells were seeded in 48 well plates at a density of 1×10^6 cells/well in 1 ml of culture media with anti-CD3 and anti-CD28 antibodies and were stimulated under indicated conditions. For macrophages, peritoneal macrophages from WT and *CSF2*$^{-/-}$ mice were harvested and seeded in 6 well plates at a density of 4×10^6 cells/well in 2 ml of culture media and were treated with or without LPS (200 ng/ml) plus IFN-γ (10 ng/ml) for 24 h. T cells or macrophages were restimulated with PMA/ionomycin/monensin for 5 h and transferred to Flow Cytometry tubes for multicolor staining for cell surface antigens and intracellular cytokines/transcription factors. Cells were first stained with FITC-anti-mouse CD4 antibody (0.25 μg/test), PE-Cy7-anti-mouse CD25 antibody (0.125 μg/test), or FITC-anti-mouse CD11b antibody (0.5 μg/test) for 30 min at 4 °C. Cells were then washed 2 times with 1xPBS (1 ml/tube), pelleted by centrifugation ($250 \times g$), and were fixed with Fixation solution (250 μl/tube; BD Biosciences) for 20 min at 4 °C. Cells were then washed 2 times with Permeabilization solution (1 ml/tube; BD Biosciences), pelleted by centrifugation ($250 \times g$), resuspended with 50 μl Permeabilization solution and stained with PE-anti-mouse GM-CSF antibody (0.125 μg/test), APC-anti-mouse IL-17a antibody (0.125 μg/test), Percp-Cy5.5-anti-mouse IFN-γ antibody (0.25 μg/test), APC-anti-mouse IL-4 antibody (0.25 μg/test), eF450-anti-mouse FOXP3 antibody (0.06 μg/test), PE-Cy7-anti-mouse NOS2 antibody (0.06 μg/test), or eF660-anti-mouse-IL-12/IL-23 p40 antibody (0.125 μg/test). Flow cytometry was performed on a FACS Calibur (BD Biosciences).

4.5. RNA isolation and quantitative real-time RT–PCR (qPCR)

Total RNA was isolated from WT, *CSF2*$^{-/-}$, *or IRAK1*$^{-/-}$ T_H0, T_H1, T_H17, or T_H-GM-CSF cells (1×10^6 cells/sample), or from WT or *CSF2*$^{-/-}$ M0 or M1 cells (4×10^6 cells/sample) using an RNeasy plus kit (QIAGEN, Valencia, CA). cDNA was generated with an oligo (dT) primer and the Superscript II system (Invitrogen, USA) followed by analysis using iCycler PCR with SYBR Green PCR master Mix (Applied Biosystems) using the primers in Supplementary Table 1. Results were normalized based on the expression of β-actin. Program was chosen to compare the CT value of target gene to housekeeping gene (β-actin) in a single sample, using the formula: $2^{-\Delta\Delta CT}$.

4.6. Immunoblotting analysis

For T cells, naïve $CD4^+$ T cells ($CD62L^+CD44^{lo}$) were prepared by FACS from spleens and lymph nodes of WT or *CSF2*$^{-/-}$ mice. The sorted cells were seeded in 24 well plates at a density of 2×10^6 cells/well in 2 ml of culture media with anti-CD3 and anti-CD28 antibodies and were stimulated under T_H1, T_H17, or T_H-GM-CSF condition for 48 h. Six wells of cells (at least 12×10^6 cells) were pooled to ensure high yields of proteins. For macrophages, peritoneal macrophages from WT or *CSF2*$^{-/-}$ mice were harvested and seeded in 6 well plates at a density of 4×10^6 cells/well in 2 ml of culture media and were stimulated under M0 or M1 condition for 24 h. Three wells of cells (12×10^6 cells) were pooled to ensure high yields of proteins. Cells were washed with cold phosphate-buffered saline and lysed for 15 min on ice in 0.5 ml of lysis buffer (50 mM Tris-HCl, pH 8.0, 280 mM NaCl, 0.5% Nonidet P-40, 0.2 mM EDTA, 2 mM EGTA, 10% glycerol, and 1 mM dithiothreitol) containing protease inhibitors. Cell lysates were clarified by centrifugation (4 °C, 15 min, $21{,}952 \times g$) and protein was subjected to 10% SDS-PAGE and immunoblotting was performed. Anti-RORγt (2 μg/ml; ThermoFisher (eBioscience)), anti-AHR (2.5 μg/ml; Abcam), anti-Ubiquitin (1:1000 dilution; ThermoFisher (Invitrogen)), anti-IRF4 (1:1000 dilution; CST), anti-p-STAT3 (1:1000 dilution; CST), anti-STAT3 (1:2000 dilution; CST), anti-β-actin (1:1000 dilution; CST), anti-IRAK1 (1:100 dilution; CST), anti-p-p65 (1:1000 dilution; CST), anti-p65 (1:1000 dilution; CST), anti-STAT1 (1:1000 dilution; CST), anti-STAT4 (1:1000 dilution; CST), anti-NOS2 (1:1000 dilution; CST), anti-IRF5 (1:1000 dilution; CST) were used according to the manufactures' instructions.

4.7. Cytokine ELISA

Naïve $CD4^+$ T cells ($CD62L^+CD44^{lo}$) were prepared by FACS from spleens and lymph nodes of WT, *IL1R1*$^{-/-}$, *ROR*$\gamma t^{-/-}$, *IL-17A*$^{-/-}$, *CSF2*$^{-/-}$, *IRAK1*$^{-/-}$, *or IRAK-M*$^{-/-}$ mice. The sorted cells were seeded in 48 well plates at a density of 1×10^6 cells/well in 1 ml of culture media with anti-CD3 and anti-CD28 antibodies and were stimulated under indicated conditions for 72 h. Supernatant from each well was collected and measured by ELISA kits. All ELISA kits were purchased from eBioscience and experiments were performed according to protocols provided by the manufacturer. Briefly, supernatants of samples were incubated in plates coated with capture antibody. Detection antibody was added after a total of five washes. Avidin-HRP was then added after a total of five washes. Plates were read at 450 nm after addition of substrate solution and stop solution. Concentration of the cytokines in samples was calculated with reference to the absorbance value obtained from the standard curve.

4.8. ChIP assay

Naive $CD4^+$ T cells from WT and *IRAK1*$^{-/-}$ mice were stimulated with IL-1β for 48 h, followed by ChIP assay manuscript. Three micrograms of an anti-NF-kB p65 antibody or isotype-matched IgG as control antibody were used in the immunoprecipitation step. PCR was used to

quantify the amount of precipitated DNA with primers flanking the p65-binding site of the CSF2 promoter region.

4.9. Isolation of peritoneal macrophages

Peritoneal cells were harvested by peritoneal lavage with of 10 ml sterile ice cold PBS. Peritoneal cells were allowed to adhere to plates for 4 h. Non-adherent cells were subsequently removed by washing with RPMI, and the adherent macrophages were refed with RPMI containing 20% calf serum and gentamicin. Purity of adherent cells (> 95%) was determined by flow cytometry following staining with using F4/80 and CD11b (BD Biosciences). Macrophages were used for experiments immediately following isolation. For some experiments macrophages were treated *ex vivo* with an M1 (10 ng/ml IFN-γ plus 200 ng/ml LPS) polarizing cocktail, or were treated with no other stimulations (M0) for the indicated time points.

4.10. Bacterial infection of mice

Citrobacter (C.) rodentium strain DBS100 (ATCC 51459) was prepared by overnight shaking at 37 °C in Luria-Bertani broth. Bacterial cultures were serially diluted and plated on MacConkey agar plates so the CFU dose administered could be confirmed. For infection, C57BL/6 mice were fasted for 8 h before oral inoculation with 2×10^9 CFU of *C. Rodentium* in a total volume of 100 µl per mouse. Mortality was monitored daily throughout the infection. Body weights were assessed at the beginning of infection and every 2 days after infection.

4.11. Endotoxin-induced sepsis shock

C57BL/6 (WT) or *CSF2*$^{-/-}$ mice were intraperitoneally administered with 800 µg E. coli-derived ultra-pure LPS or PBS. Survival was monitored continuously. Mice were euthanized at a humane end point after loss of self-righting (capability to right itself after falling) and insensitivity to touch were noted. For serum collection, mice were injected i. p. with 800 µg LPS and sera were collected 6 h later. Spleens were collected as well.

4.12. T cell-transfer colitis

Purified CD4$^+$CD45RB^{hi} T cells from C57BL/6J (WT) mice and age- and sex-matched *CSF2*$^{-/-}$ or *IL1R1*$^{-/-}$ mice were injected intraperitoneally into female 8-12-week-old *Rag1*$^{-/-}$ recipients (5×10^5 cells per mouse in 200 µl sterile PBS per injection). Mice were weighed every week throughout the course of experiments and were sacrificed after 5 weeks for evaluation of disease severity.

4.13. DSS colitis model

Female C57BL/6J (WT) mice and *CSF2*$^{-/-}$ mice aged 8–12 weeks were used to generate DSS-induced chronic colitis model. Mice were administered 2.5% DSS in their drinking water for 5 days, followed by 7 days of the administration of distilled water. This cycle was repeated 3 times. Mice were monitored for weight changes, diarrhea, bloody stools, and overall health. Mice were removed from the study when their body weight loss exceeded 25% of their original body weight and counted as death. Disease activity index (DAI) score was calculated as sum of the weight loss score (0–4), the diarrheal score (0–4) and the hematochezia score (0–4) and was monitored daily.

4.14. Tissue collection and histology

Colon tissues (including three segments: proximal, middle and distal) were dissected from mice, fixed in 10% phosphate-buffered formalin, and then processed for paraffin sections. Sections (5 µm) of tissue samples were stained with hematoxylin and eosin (H&E) for evaluation of tissue pathology. Histological score was evaluated as follows: submucosa damage, 0; normal or widely scattered leukocytes, 1; focal aggregates of leukocytes, 2; diffuse leukocyte infiltration with expansion of submucosa, 3; diffuse leukocyte infiltration. The histological scores were determined for each segment, and the total score was calculated as the sum of the histological scores in all segments. All of the slides were read and scored by an experienced pathologist without previous knowledge of the type of treatment. The proximal part of colon was collected for tissue RNA extraction.

4.15. Immunofluorescence

Sections were deparaffinized in xylene and dehydrated in ethanol. Primary antibody was incubated overnight at 4 °C and secondary biotinylated antibody was detected with streptavidin-HRP or fluorescent probe-conjugated antibody. Sections were development using a DAB peroxidase substrate kit (BioGenex). For immunofluorescence, media counting with DAPI was used. Images were acquired using a Nikon Eclipse NE and with NIS elements BR software.

4.16. Statistical analysis

The results are shown as means ± SD. and statistical analysis was performed using Student's t-test. Where more than two groups were compared, one-way ANOVA with a Bonferroni's correction was performed; Student's t-test was used to determine the difference in survival rate. P values < 0.05 were considered statistically significant.

Conflicts of interest

The authors declare that they have no competing interests.

Acknowledgement

Huabao Xiong was supported by NIH funding RO1AI104688. Peter. S Heeger was supported by RO1AI132405 and RO1AI071185.

Appendix A. Supplementary data

Supplementary data to this article can be found online at https://doi.org/10.1016/j.jaut.2019.04.010.

References

[1] A.W. Burgess, D. Metcalf, The nature and action of granulocyte-macrophage colony stimulating factors, Blood 56 (1980) 947–958.
[2] J.A. Hamilton, Colony-stimulating factors in inflammation and autoimmunity, Nat. Rev. Immunol. 8 (2008) 533–544.
[3] B. Becher, S. Tugues, M. Greter, GM-CSF: from growth factor to central mediator of tissue inflammation, Immunity 45 (2016) 963–973.
[4] A. Shiomi, T. Usui, Pivotal roles of GM-CSF in autoimmunity and inflammation, Mediat. Inflamm. 2015 (2015) 568543.
[5] A. Mortha, et al., Microbiota-dependent crosstalk between macrophages and ILC3 promotes intestinal homeostasis, Science 343 (2014) 1249288.
[6] R. Li, et al., Proinflammatory GM-CSF-producing B cells in multiple sclerosis and B cell depletion therapy, Sci. Transl. Med. 7 (2015) 310ra166.
[7] A. Sheih, W.C. Parks, S.F. Ziegler, GM-CSF produced by the airway epithelium is required for sensitization to cockroach allergen, Mucosal Immunol. 10 (2017) 705–715.
[8] L. Egea, et al., GM-CSF produced by nonhematopoietic cells is required for early epithelial cell proliferation and repair of injured colonic mucosa, J. Immunol. 190 (2013) 1702–1713.
[9] L. Codarri, et al., RORgammat drives production of the cytokine GM-CSF in helper T cells, which is essential for the effector phase of autoimmune neuroinflammation, Nat. Immunol. 12 (2011) 560–567.
[10] M. El-Behi, et al., The encephalitogenicity of T(H)17 cells is dependent on IL-1- and IL-23-induced production of the cytokine GM-CSF, Nat. Immunol. 12 (2011) 568–575.
[11] W. Sheng, et al., STAT5 programs a distinct subset of GM-CSF-producing T helper cells that is essential for autoimmune neuroinflammation, Cell Res. 24 (2014) 1387–1402.
[12] A.L. Croxford, S. Spath, B. Becher, GM-CSF in neuroinflammation: licensing

myeloid cells for tissue damage, Trends Immunol. 36 (2015) 651–662.
[13] C.L. Langrish, et al., IL-23 drives a pathogenic T cell population that induces autoimmune inflammation, J. Exp. Med. 201 (2005) 233–240.
[14] I.L. McWilliams, R. Rajbhandari, S. Nozell, E. Benveniste, L.E. Harrington, STAT4 controls GM-CSF production by both Th1 and Th17 cells during EAE, J. Neuroinflammation 12 (2015) 128.
[15] J.R. Lukens, M.J. Barr, D.D. Chaplin, H. Chi, T.D. Kanneganti, Inflammasome-derived IL-1beta regulates the production of GM-CSF by CD4(+) T cells and gammadelta T cells, J. Immunol. 188 (2012) 3107–3115.
[16] R. Noster, et al., IL-17 and GM-CSF expression are antagonistically regulated by human T helper cells, Sci. Transl. Med. 6 (2014) 241ra280.
[17] J. Rasouli, et al., Expression of GM-CSF in T cells is increased in multiple sclerosis and suppressed by IFN-beta therapy, J. Immunol. 194 (2015) 5085–5093.
[18] E.E. Kara, et al., CCR2 defines in vivo development and homing of IL-23-driven GM-CSF-producing Th17 cells, Nat. Commun. 6 (2015) 8644.
[19] K. Hirota, et al., Fate mapping of IL-17-producing T cells in inflammatory responses, Nat. Immunol. 12 (2011) 255–263.
[20] F.C. Kurschus, et al., Genetic proof for the transient nature of the Th17 phenotype, Eur. J. Immunol. 40 (2010) 3336–3346.
[21] Y.K. Lee, et al., Late developmental plasticity in the T helper 17 lineage, Immunity 30 (2009) 92–107.
[22] N. Gagliani, et al., Th17 cells transdifferentiate into regulatory T cells during resolution of inflammation, Nature 523 (2015) 221–225.
[23] C.E. Zielinski, et al., Pathogen-induced human TH17 cells produce IFN-gamma or IL-10 and are regulated by IL-1beta, Nature 484 (2012) 514–518.
[24] M. DuPage, J.A. Bluestone, Harnessing the plasticity of CD4(+) T cells to treat immune-mediated disease, Nat. Rev. Immunol. 16 (2016) 149–163.
[25] Ivanov IIet al., The orphan nuclear receptor RORgammat directs the differentiation program of proinflammatory IL-17+ T helper cells, Cell 126 (2006) 1121–1133.
[26] M. Veldhoen, et al., The aryl hydrocarbon receptor links TH17-cell-mediated autoimmunity to environmental toxins, Nature 453 (2008) 106–109.
[27] M. Ciofani, et al., A validated regulatory network for Th17 cell specification, Cell 151 (2012) 289–303.
[28] S. Gottipati, N.L. Rao, W.P. Fung-Leung, IRAK1: a critical signaling mediator of innate immunity, Cell. Signal. 20 (2008) 269–276.
[29] K. Kobayashi, et al., IRAK-M is a negative regulator of Toll-like receptor signaling, Cell 110 (2002) 191–202.
[30] P.L. Podolin, et al., Attenuation of murine collagen-induced arthritis by a novel, potent, selective small molecule inhibitor of IkappaB Kinase 2, TPCA-1 (2-[(aminocarbonyl)amino]-5-(4-fluorophenyl)-3-thiophenecarboxamide), occurs via reduction of proinflammatory cytokines and antigen-induced T cell Proliferation, J. Pharmacol. Exp. Ther. 312 (2005) 373–381.
[31] W. O'Connor Jr.et al., A protective function for interleukin 17A in T cell-mediated intestinal inflammation, Nat. Immunol. 10 (2009) 603–609.
[32] T. Griseri, B.S. McKenzie, C. Schiering, F. Powrie, Dysregulated hematopoietic stem and progenitor cell activity promotes interleukin-23-driven chronic intestinal inflammation, Immunity 37 (2012) 1116–1129.
[33] T. Griseri, et al., Granulocyte macrophage colony-stimulating factor-activated eosinophils promote interleukin-23 driven chronic colitis, Immunity 43 (2015) 187–199.
[34] F.O. Martinez, S. Gordon, The M1 and M2 paradigm of macrophage activation: time for reassessment, F1000Prime Rep 6 (2014) 13.
[35] T. Krausgruber, et al., IRF5 promotes inflammatory macrophage polarization and TH1-TH17 responses, Nat. Immunol. 12 (2011) 231–238.
[36] M.J. McGeachy, et al., The interleukin 23 receptor is essential for the terminal differentiation of interleukin 17-producing effector T helper cells in vivo, Nat. Immunol. 10 (2009) 314–324.
[37] J. Bilsborough, S.R. Targan, S.B. Snapper, Therapeutic targets in inflammatory bowel disease: current and future, Am J Gastroenterol Suppl 3 (2016) 27–37.
[38] J. Galvez, Role of Th17 cells in the pathogenesis of human IBD, ISRN Inflamm 2014 (2014) 928461.
[39] N. Komatsu, et al., Pathogenic conversion of Foxp3+ T cells into TH17 cells in autoimmune arthritis, Nat. Med. 20 (2014) 62–68.
[40] L. Cosmi, et al., Evidence of the transient nature of the Th17 phenotype of CD4+CD161+ T cells in the synovial fluid of patients with juvenile idiopathic arthritis, Arthritis Rheum. 63 (2011) 2504–2515.
[41] L. Cosmi, L. Maggi, V. Santarlasci, F. Liotta, F. Annunziato, T helper cells plasticity in inflammation, Cytometry 85 (2014) 36–42.
[42] M. Windheim, M. Stafford, M. Peggie, P. Cohen, Interleukin-1 (IL-1) induces the Lys63-linked polyubiquitination of IL-1 receptor-associated kinase 1 to facilitate NEMO binding and the activation of IkappaBalpha kinase, Mol. Cell Biol. 28 (2008) 1783–1791.
[43] C. Pearson, et al., ILC3 GM-CSF production and mobilisation orchestrate acute intestinal inflammation, Elife 5 (2016) e10066.
[44] E. Zigmond, et al., Ly6C hi monocytes in the inflamed colon give rise to proinflammatory effector cells and migratory antigen-presenting cells, Immunity 37 (2012) 1076–1090.
[45] M. Noguchi, N. Hiwatashi, Z.X. Liu, T. Toyota, Increased secretion of granulocyte-macrophage colony-stimulating factor in mucosal lesions of inflammatory bowel disease, Digestion 63 (Suppl 1) (2001) 32–36.
[46] J. Dabritz, Granulocyte macrophage colony-stimulating factor and the intestinal innate immune cell homeostasis in Crohn's disease, Am. J. Physiol. Gastrointest. Liver Physiol. 306 (2014) G455–G465.